Thermomechanical couplings in shape memory alloy materials

D.Soldatos[a], S. P. Triantafyllou[b], V. P. Panoskaltsis[a]

[a] Department of Civil Engineering, Demokritos University of Thrace, University Campus

Xanthi-Kimmeria, 67100 Xanthi, GREECE

[b]Department of Civil Engineering, University of Nottingham, University Park, NottighamNG7

2RD, UK

AbstractIn this work we address several theoretical and computational issues which are related to the thermomechanical modeling of shape memory alloy materials. More specifically, in this paper we revisit a non-isothermal version of the theory of large deformation generalized plasticity which is suitable for describing the multiple and complex mechanisms occurring in these materials during phase transformations. We also discuss the computational implementation of a generalized plasticity based constitutive model and we demonstrate the ability of the theory in simulating the basic patterns of the experimentally observed behavior by a set of representative numerical examples.

Keywords Shape memory alloys - Shape memory effect - Pseudoelasticity- Generalized plasticity - Invariance - balance energy equation - Thermomechanical state equations – Isothermal split - Thermomechanical couplings

1 Introduction

Shape Memory Alloys (SMAs) are an intriguing class of metal alloys with the ability to undergo severe deformations and then recover their original shape. This can occur either under the action of a thermomechanical cycle, with the corresponding response termed as shape memory effect or a stress cycle within some appropriate temperature limits (pseudoelasticity). Two are the fundamental mechanisms underlying this recovery. The first one is a diffusionless transformation between the high ordered austenite phase (parent phase) and the less ordered martensite (product) phase. The second evolves through the reorientation (detwinning) of the martensite variants. These transformations are termed as martensitic and may be met also in other metallic materials such as carbon steels and invar alloys.

Due to these properties SMAs are being increasingly used in several innovating applications which are met at almost all engineering fields. Thus, there is a pressing need for simulation tools that can accurately describe their experimentally observed behavior, especially under complex states of stress and temperature.

For the past three decades there has been substantial activity to model martensitic transformations in shape memory alloys within a fully coupled thermomechanical framework. This approach relies on the use of the so-called non-equilibrium (or irreversible) thermodynamics. Within this approach, among others, Müller [28], Raniecki et al. [43], Huo and Müller [15], Raniecki and Lexcellent [44], Leclercq and Lexcellent [18], Boyd and Lagoudas [8], Lagoudas et al. [17], Peyroux et al. [40], Raniecki and Lexcellent [45], Müller and Bruhns [29], Ziołkowski [57] Christ and Reese [9],

2

48 Thamburaja [52], Morin et al. [27], Yu et al. [55] have proposed models based on the use

49 of a set of thermomechanical equations describing thekinematics of the martensitic

50 transformations. The constitutive equations are developed in a non-linear manner on the

51 basis of a free energy driving force and the laws of thermodynamics.

52   An alternative approach is the employment of plastic flow theories. Such an approach

53 is thermodynamically consistent and may furnish a concrete micromechanical

54 justification - see, e.g., the ideas exposed in the book by Smallman and Bishop ([50, pp.

55 278-280]); see also the concise discussion given in Panoskaltsis et al. [36]. On the basis

56 of this idea, Anand and Gurtin [2], by following the equilibrium theory of austenite -

57 martensite phase transitions of Ball and James [6], proposed a three-dimensional crystal

58 model which was able to reproduce the pseudoelastic response of SMAs under isothermal

59 and non-isothermal conditions. Related is the thermomechanical model by Lu and Weng

60 [20] - see also Yin and Weng [54] - where a set of explicit constitutive equations which

61 provide a direct link between the applied stress and the evolution of the product phase

62 during martensitic transformations, and between the stress and the overall strain of the

63 transforming system, is discussed.

64   Nevertheless, modeling a polycrystalline body remains a challenging task. Even in the

65 single crystal there exist 192 transformation systems (see Ball and James [6]; Anand and

66 Gurtin [2]; Yin and Weng [54]) and accordingly the number of active transformation

67 systems can be immense. Thus, a macroscopic approach within the context of plasticity

68 theories seems also attractive. Moreover, the macroscopic approach offers several

69 computational advantages since, as it is noted by Thamburaja [52], the numerical

70 implementation of macroscopic models is easier than that of crystal models, while the

71 numerical simulations involving macroscopic models are computationally more efficient.

72   An interesting approach within the context of macroscopic theories of plasticity is the

73 one suggested by Lubliner and Auricchio [22] - see also the related work by Panoskaltsis

74 [32]; Panoskaltsis et al. [33 - 39] who developed a three-dimensional thermomechanical

75 constitutive model, based on non-isothermal generalized plasticity theory (Lubliner [21]).

76 Generalized plasticity is a general theory of rate-independent inelastic behavior which is

77 physically motivated by loading-unloading irreversibility and is mathematically founded

78 on set theory and topology. This general mathematical foundation provides the theory

79 with the ability to deal with "non-standard" cases such as non-connected elastic domains,

80 which is exactly the challenge in modeling SMAs.

81   The basic objective of this work is to revisit the previous work by Lubliner and Auricchio

82 [22] and Panoskaltsis et al. [36] - see also [33, 34] and to provide a general

83 thermomechanical framework, which in turn may constitute a basis for the derivation of

84 constitutive models for SMAs. Further to the aforementioned endeavors, the present

85 approach establishes the theory in a covariant setting and utilizes the modern invariance

86 (symmetry) principles for the derivation of the thermomechanical state equations. On the

87 computational side, novel aspects include: (1) The derivation of a (local) time integration

88 algorithm within the context of an isothermal operator split and (2) the numerical

89 simulation of non-conventional patterns of material response, where phase transformations

90 may be retarded or even inhibited due to self-heating/cooling effects.

91   This paper is organized as follows: In Section 2, we revisit the general multi-surface

92 formulation of non-isothermal generalized plasticity developed in Panoskaltsis et al. [33]

4

93 and we extend it in a covariant setting; we also render the theory fully covariant - see, e.g.,

94 Marsden and Hughes [23, pp. 202-203]- upon studying the invariance properties of the

95 local balance of energy under general spatial transformations. In Section 3, as an

96 application we present a material model; this model constitutes a straight forward extension

97 to the non-isothermal regime of a model which has been recently discussed by the authors

98 in [36]. The extension is based on some basic results underlying the thermomechanical

99 response of an SMA material developed in Raniecki et al. [43], Raniecki and Lexcellent

100 [44] and Müller and Bruhns [29]. Finally, in Section 4 we discuss the computational

101 aspects which are related to the numerical implementation of the model and we present a

102 set of representative numerical examples.

103

104

105 **2   Constitutive theory**

106

107 *2.1 Review of the basic equations*

108

109 Similar to our previous work [36], a homogeneous body is considered, undergoing phase

110 transformations and occupying a region Ω in the ambient space $S = R^3$, with points X

111 labeled by $\left(X^1, X^2, X^3 \right)$. The region Ω is identified by the body material (reference)

112 configuration. A motion of the body within the ambient space S is defined accordingly as

113 the time dependent mapping **x**:

$$\mathbf{x} : \Omega \rightarrow S, \ \mathbf{x} = \mathbf{x_t} = \mathbf{x}(\mathbf{X}, t) \tag{1}$$

115 which maps the points $\mathbf{X}$ of the material configuration onto the points $\mathbf{x}$ of the spatial

116 (current) configuration. Then the deformation gradient is defined as the tangent map of

117 (1), i.e.

118
$$\mathbf{F} = T\mathbf{x} = \frac{\partial \mathbf{x}(\mathbf{X},t)}{\partial \mathbf{X}},$$

119 and the material (Green-St. Venant) strain tensor is defined as:

120
$$\mathbf{E} = \frac{1}{2}(\mathbf{C} - \mathbf{I}),$$

121 where $\mathbf{C}$ is the right Cauchy-Green deformation tensor defined as $\mathbf{C} = \mathbf{F}^{\mathrm{T}}\mathbf{F}$ and $\mathbf{I}$ is the

122 unit rank-2 tensor. Following [36], we assume that the basic kinematic assumption is based

123 on an additive decomposition of the strain tensor $\mathbf{E}$ into elastic $\mathbf{E}_e$ and inelastic

124 (transformation induced) $\mathbf{E}_{\mathrm{Tr}}$ parts, i.e.

125
$$\mathbf{E} = \mathbf{E}_e + \mathbf{E}_{\mathrm{Tr}}, \tag{2}$$

126 where $\mathbf{E}_{\mathrm{Tr}}$ represents inelastic deformation induced by generation, growth and annihilation

127 of the austenitic - martensitic fine structure (see, e.g., [6]) and defines an inelastically

128 deformed (intermediate) configuration and $\mathbf{E}_e$ represents elastic deformation due to

129 stretching and rotation of the crystal lattice.

130   Since we deal with an internal variable theory, it is assumed that the local

131 thermomechanical state in a body - see, e.g., [21, 22] - is determined uniquely by the

132 couple $(\mathbf{G},\mathbf{Q})$ where $\mathbf{G}$ - belonging to a space G - stands for the vector of the controllable

133 state variables and $\mathbf{Q}$ -belonging to a space Q - stands for the vector of the internal

134 variables. According to the ideas presented in the review paper of Naghdi [30] the present

135 work is based on a referential (material) approach within a strain-space formulation.

6

136 Accordingly, **G** may be identified by the couple (**E**,T), where T is the (absolute)

137 temperature. In view of the additive decomposition (2), the internal variable vector may

138 be assumed to be composed by the transformation strain tensor $\mathbf{E_{Tr}}$ and an additional

139 internal variable vector **Z**.

140 The mathematical foundations of generalized plasticity - see Lubliner [21] - rely

141 crucially on a shift of emphasis from the yield surface concept to that of the elastic range.

142 This is defined at any material state as the region in the strain-temperature space

143 comprising the values of **G**'s that can be attained elastically - i.e. with no change in the

144 internal variables $(\mathbf{E_{Tr}},\mathbf{Z})$ - from the current strain-temperature point. The boundary of

145 this set may be defined as a loading surface (see further [21]). In turn a material state may

146 be defined as elastic if it is an interior point of its elastic range and inelastic if it is a

147 boundary point of its elastic range. It should be added that the notion of process is

148 introduced implicitly here. In a recent paper Panoskaltsis et al. [34] - see also [33] - argued

149 that for a material undergoing phase transformations the loading surface may be assumed

150 to be defined by a set of *n* smooth surfaces which are defined by expressions of the form

151
$$F_\alpha(\mathbf{E},\mathrm{T},\mathbf{E_{Tr}},\mathbf{Z}) = 0, \quad \alpha=1,2,...,n.$$

152 Each of these surfaces is associated with a particular transformation mechanism - denoted

153 here symbolically by α - which may be active at the current state. It is further assumed

154 that each equation $F_\alpha(\mathbf{E},\mathrm{T},\mathbf{E_{Tr}},\mathbf{Z}) = 0$ defines independent (non-redundant) active

155 surfaces at the current value of (**E**,T) and that the elastic range is a convex set. Then, on

156 the basis of the defining property of an inelastic state and the irreversibility of an inelastic

157 process from such a state it can be shown (see [21]; see also [33, 34] for the case of SMAs)

158 that the rate equations underlying the evolution of the internal variables may be stated as

$$\dot{\mathbf{E}}_{\mathrm{Tr}} = \sum_{\alpha=1}^{n} H_{\alpha}(\mathbf{E}, \mathrm{T}, \mathbf{E}_{\mathrm{Tr}}, \mathbf{Z}) \mathbf{L}_{\alpha}(\mathbf{E}, \mathrm{T}, \mathbf{E}_{\mathrm{Tr}}, \mathbf{Z}) \langle L_{\alpha} \rangle,$$

159 $\qquad\qquad$ (3)

$$\dot{\mathbf{Z}} = \sum_{\alpha=1}^{n} H_{\alpha}(\mathbf{E}, \mathrm{T}, \mathbf{E}_{\mathrm{Tr}}, \mathbf{Z}) \mathbf{M}_{\alpha}(\mathbf{E}, \mathrm{T}, \mathbf{E}_{\mathrm{Tr}}, \mathbf{Z}) \langle L_{\alpha} \rangle$$

160 where <·> stands for the Macaulay bracket which is defined as

161
$$\langle x \rangle = \begin{cases} x & \text{if } x > 0 \\ 0 & \text{if } x \le 0 \end{cases},$$

162 and the H_{α}'s stand for scalar functions which enforce the defining property of an inelastic

163 state. Accordingly, the values of H_{α}'s must be positive at any inelastic state and zero at

164 any elastic one. Finally, $\mathbf{L}_{\alpha}$ and $\mathbf{M}_{\alpha}$ represent non-vanishing functions, which are

165 associated with the properties of the phase transformation connected with the part of the

166 loading surface defined by $F_{\alpha} = 0$, while the L_{α}'s stand for the non-isothermal loading

167 rates which are defined to be

168
$$L_{\alpha} = \frac{\partial F_{\alpha}}{\partial \mathbf{E}} : \dot{\mathbf{E}} + \frac{\partial F_{\alpha}}{\partial \mathrm{T}} \dot{\mathrm{T}}.$$

169 From Eqs. (3), one can deduce directly the loading-unloading criteria for the proposed

170 formulation, which may be systematically formulated as [34], in terms of the sets

171
$$\mathrm{J}_{\mathrm{adm}} = \{ \beta \in \{1, 2, \dots, n\} / H_{\beta} > 0 \}$$

172 and

173
$$\mathrm{J}_{\mathrm{act}} = \{ \beta \in \mathrm{J}_{\mathrm{adm}} / L_{\beta} > 0 \},$$

174 as follows

8

$$
\begin{cases}
\text{If } J_{adm} = \varnothing : & \text{elastic state.} \\
\text{If } J_{adm} \neq \varnothing \text{ and } J_{act} = \varnothing : & \\
\quad \text{i. If } L_\beta < 0 \text{ for all } \beta \in J_{adm}: & \text{elastic unloading,} \\
\quad \text{ii. If } L_\beta = 0 \text{ for at least one } \beta \in J_{adm}: & \text{neutral loading,} \\
\text{If } J_{adm} \neq \varnothing \text{ and } J_{act} \neq \varnothing : & \text{inelastic loading.}
\end{cases}
\tag{4}
$$

175

176 An equivalent assessment of the governing equations in the spatial configuration can be

177 done on the basis of a push-forward operation (see, e.g., Marsden and Hughes [23, pp.67-

178 68]; Stumpf and Hoppe [51]; Holzapfel [14, pp. 82-84]) to the basic equations. For

179 instance, by performing a push-forward operation onto Eq. (2) the latter can be written in

180 the form

181
$$
\mathbf{e} = \mathbf{e}_{\mathbf{e}} + \mathbf{e}_{\mathbf{Tr}},
$$

182 where $\mathbf{e}$ is the spatial (Almansi) strain tensor, defined as the push-forward of $\mathbf{E}$, that is

183 $\mathbf{e} = \mathbf{F}^{-T}\mathbf{E}\mathbf{F}^{-1}$, and $\mathbf{e}_{\mathbf{e}}$, $\mathbf{e}_{\mathbf{Tr}}$ are the corresponding elastic and transformation induced parts. In

184 a similar manner the rate equations for the evolution of the internal variables in the spatial

185 configuration read

186
$$
L_{\mathbf{V}}\mathbf{e}_{\mathbf{Tr}} = \sum_{\alpha=1}^{n} h_\alpha(\mathbf{e}, T, \mathbf{e}_{\mathbf{Tr}}, \mathbf{z}, \mathbf{F})\mathbf{l}_\alpha(\mathbf{e}, T, \mathbf{e}_{\mathbf{Tr}}, \mathbf{z}, \mathbf{F})\langle l_\alpha \rangle,
$$
$$
L_{\mathbf{V}}\mathbf{z} = \sum_{\alpha=1}^{n} h_\alpha(\mathbf{e}, T, \mathbf{e}_{\mathbf{Tr}}, \mathbf{z}, \mathbf{F})\mathbf{m}_\alpha(\mathbf{e}, T, \mathbf{e}_{\mathbf{Tr}}, \mathbf{z}, \mathbf{F})\langle l_\alpha \rangle,
\tag{5}
$$

187 where $\mathbf{z}$ stands for the push-forward of the internal variable vector, and $L_{\mathbf{V}}(\cdot)$ stands for

188 the Lie derivative (see further [23, pp.93-104]; [51]; [14, pp. 106-108]), defined as the

189 convected derivative relative to the spatial configuration. Finally, the h_α's stand for the

190 expression of the (scalar invariant) functions H_α in terms of the spatial variables

191 $(\mathbf{e}, T, \mathbf{e}_{\mathbf{Tr}}, \mathbf{z})$ and the deformation gradient $\mathbf{F}$, $\mathbf{l}_\alpha$ and $\mathbf{m}_\alpha$ stand for the push-forward of the

192   functions $\mathbf{L}_\alpha$ and $\mathbf{M}_\alpha$ respectively and the l_α's stand for the (scalar invariant) loading

193   rates which in the spatial configuration are given as

194
$$l_\alpha = \frac{\partial f_\alpha}{\partial \mathbf{e}}:\mathrm{L_v}\mathbf{e} + \frac{\partial f_\alpha}{\partial \mathrm{T}}\dot{\mathrm{T}}.$$

195   In this equation f_α is the expression for the loading surface associated with the index α in

196   terms of the spatial variables. The (spatial) loading-unloading criteria follow naturally from

197   Eqs. (5) as

198
$$\begin{cases} \text{If } \mathrm{j_{adm}} = \varnothing: & \text{elastic state.} \\ \text{If } \mathrm{j_{adm}} \neq \varnothing \text{ and } \mathrm{j_{act}} = \varnothing: & \\ \quad \text{i. If } l_\beta < 0 \text{ for all } \alpha \in \mathrm{j_{adm}}: & \text{elastic unloading,} \\ \quad \text{ii. If } l_\beta = 0 \text{ for at least one } \alpha \in \mathrm{j_{adm}}: & \text{neutral loading,} \\ \text{If } \mathrm{j_{adm}} \neq \varnothing \text{ and } \mathrm{j_{act}} \neq \varnothing: & \text{inelastic loading.} \end{cases}$$

199   where the sets $\mathrm{j_{adm}}$ and $\mathrm{j_{act}}$ are now defined in terms of the spatial variables as

200    $\mathrm{j_{adm}} = \{\beta \in \{1,2,...,\mathrm{n}\}/h_\beta > 0\}$ and $\mathrm{j_{act}} = \{\beta \in \mathrm{J_{adm}}/l_\beta > 0\}$.

201

202

203   *2.2 Covariant constitutive theory*

204

205   In the classical literature of the thermomechanical modeling of SMAs it is common to use

206   approaches which are based on the second law of thermodynamics for the derivation of the

207   thermomechanical state equations. An alternative formulation may be established on the

208   basis of an invariance (symmetry) principle (see, e.g., Marsden and Hughes [23, pp. 154-

209   176, 199-204, 275-288]; Yavari et al. [53]; see also the philosophical reflections given in

210   Earman [10] and the recent account by Ganghoffer [12]). Such an approach is based on the

211 exploitation of the invariance properties of a quantity underlying the response of a

212 dynamical system under the action of some group of transformations. For instance,

213 Marsden and Hughes in [23, pp. 199-204], derived the classical stress-deformation and

214 entropy-temperature relations for an elastic material by postulating the invariance of the

215 local form of the referential energy balance equation under the superposition of a group of

216 spatial transformations.

217 The basic objective of this Section is to revisit the approach of Marsden and Hughes in

218 [23] and introduce it within a shape memory alloy behavior setting. In particular, the

219 derivation of both the stress tensor and the specific entropy from the Helmholtz free energy

220 is demonstrated, when the *local form of the material balance of energy equation is*

221 *invariant* under superposition of a special group of transformations. This group consists of

222 *arbitrary spatial diffeomorphisms*, that is transformations of the ambient space *which may*

223 *change the spatial strain tensor* (**e**). It is noted that in order to change the local

224 thermomechanical state such a group of transformations is not enough since this will

225 change the mechanical state, but not the thermomechanical one. Therefore, in addition we

226 need also a transformation of the temperature, that is a diffeomorphism of R^+ (see the

227 footnote in p. 202 in Marsden and Hughes [23]). The simplest case for such a

228 diffeomorphism is a *temperature rescaling*.

229 It is noted that, unlike the original approach by Marsden and Hughes [23] where the

230 ambient space is considered to be a Riemannian manifold, within the present approach this

231 space is the (rigid) Euclidean space. In this case the basic axioms of Marsden and Hughes

232 [23, pp. 202-203], for the material which obeys the rate Eqs. (3) (or equivalently Eqs. (5))

233 in the course of phase transformations, can be stated as follows:

234   *Axiom 1:* At the material point $\mathbf{X}$ and a given thermomechanical process $\mathbf{G}$ there exists a

235   scalar function E of the state variables $(E = E(\mathbf{E}, \mathrm{T}, \mathbf{E_{Tr}}, \mathbf{Z}))$ such as the energy balance

236   equation holds, that is

237

$$\rho_{ref}\dot{E} + DIV\mathbf{H} = \mathbf{S} : \dot{\mathbf{E}} + \rho_{ref}R,$$

238   where ρ_{ref} is the mass density in the material configuration, $\mathbf{S}$ is the second Piola-Kirchhoff

239   stress tensor, $\mathbf{H}$ is the heat flux vector and R is the heat supply per unit mass. By introducing

240   the Helmholtz free energy function Ψ, which is obtained by the usual Legendre

241   transformation $\Psi = E - N\mathrm{T}$, where N is the specific entropy $(N = N(\mathbf{E}, \mathrm{T}, \mathbf{E_{Tr}}, \mathbf{Z}))$, the

242   local form of the energy balance can be written in the form

243

$$\rho_{ref}(\dot{\Psi} + \dot{N}\mathrm{T} + N\dot{\mathrm{T}}) + DIV\mathbf{H} = \mathbf{S} : \dot{\mathbf{E}} + \rho_{ref}R, \qquad (6)$$

244   where $DIV(\cdot)$ stands for the divergence operator in the material description.

245   *Axiom 2:* We denote by g and q the spaces of the control variables in the spatial

246   configuration - that is the spaces G and Q, "as seen" in the spatial configuration - and by

247   ω the set of the C^{S} scalar fields in the spatial configuration, and we assume the existence

248   of a map $\hat{\hat{\Psi}} : (S, g, q, R^+) \rightarrow \omega$ such that for any diffeomorphism $(\xi, \delta) : (S, R^+) \rightarrow (S, R^+)$,

249

$$\hat{\Psi}(\mathbf{x}, \mathbf{e}, \mathrm{T}, \mathbf{e_{Tr}}, \mathbf{z}) = \hat{\hat{\Psi}}(\xi \circ \mathbf{x}, \xi_* \mathbf{e}, \delta\mathrm{T}, \mathbf{e_{Tr}}(\xi_* \mathbf{e}, \delta\mathrm{T}), \mathbf{z}(\xi_* \mathbf{e}, \delta\mathrm{T}), \delta).$$

250   *Axiom 3:* For curves $\xi_t : S \rightarrow S$ and $\delta_t(x) \in R^+$, assume that $\mathbf{x_t}' = \xi_t \circ \mathbf{x_t}$, $\mathrm{T_t}' = \delta_t \mathrm{T_t}$ satisfy

251   the balance of energy, that is

252

$$\rho_{ref}'(\dot{\Psi}' + \dot{N}'\mathrm{T}' + N'\dot{\mathrm{T}}') + DIV\mathbf{H}' = \mathbf{S}' : \dot{\mathbf{E}}' + \rho_{ref}'R'. \qquad (7)$$

253 where it has been further assumed that ρ_{ref}, Ψ, N and the F_α's are transformed as scalars,

254 the heat flux vector is transformed as $\mathbf{H_t}' = \delta_t \xi_{t*} \mathbf{H_t}$ and the *"apparent heat supply" due to*

255 *entropy production* $R_t' - T_t \dot{N}_t'$, is transformed as $R_t' - T_t' \dot{N}_t' = \delta_t (R_t - T_t \dot{N}_t)$.

256 In this case the internal variables $\mathbf{e_{tr}}$ and $\mathbf{z}$, under the application of the spatial

257 diffeomorphism and the temperature rescaling, *do not follow their own mode of evolution*

258 *since are always related to the spatial strain tensor* $\mathbf{e}$ *and the temperature* T *by Eqs.* (5).

259 Moreover, and more importantly it is noted that for both $\mathbf{x_t}$ and $\mathbf{x_t'} = \xi_t \circ \mathbf{x_t}$, the balance of

260 energy equation is written *at the same material point* $\mathbf{X}$. Accordingly, the transformed

261 values of the strain and temperature rates in the primed system- see also [53] - will be given

262 as

$$\dot{\mathbf{E}}_t' = T \xi_t \circ \dot{\mathbf{E}}_t + \frac{\partial \xi}{\partial t} \circ \mathbf{E_t},$$

263 (8)

$$\dot{T}_t' = \delta \dot{T}_t + \frac{\partial \delta}{\partial t} T_t.$$

264 The invariance properties of the balance of energy equation are exploited as in Marsden

265 and Hughes [23] by evaluating Eq. (7) at time t_0, when $\xi|_{t=t_0} = \mathbf{1}$ (identity), $\mathbf{w} = \frac{\partial \xi}{\partial t}\bigg|_{t=t_0}$ and

266 $\delta|_{t=t_0} = 1$, $u = \frac{\partial \delta}{\partial t}\bigg|_{t=t_0}$ where u is the velocity of δ at t_0.

267 The time derivative of the transformed Helmholtz free energy in this case reads

$$\dot{\Psi}'\bigg|_{t=t_0} = \frac{\partial \Psi'}{\partial \mathbf{E}'} : \dot{\mathbf{E}}'\bigg|_{t=t_0} + \frac{\partial \Psi'}{\partial T'} : \dot{T}'\bigg|_{t=t_0} + \frac{\partial \Psi'}{\partial \mathbf{E_{Tr}'}} : \dot{\mathbf{E}}_{Tr}'\bigg|_{t=t_0} + \frac{\partial \Psi'}{\partial \mathbf{Z}'} : \dot{\mathbf{Z}}'\bigg|_{t=t_0}.$$

268 (9)

269 By means of Eqs. (8) the time derivatives $\dot{\mathbf{E}}'\big|_{t=t_0}$ and $\dot{T}'\big|_{t=t_0}$ are found to be

13

$$\dot{\mathbf{E}}'\Big|_{t=t_0} = \dot{\mathbf{E}} + \mathbf{w} \circ \mathbf{E},$$

270

$$\dot{\mathrm{T}}'\Big|_{t=t_0} = \dot{\mathrm{T}} + u\mathrm{T}. \tag{10}$$

271 The time derivatives $\dot{\mathbf{E}}'_{\mathbf{Tr}}\big|_{t=t_0}$ and $\dot{\mathbf{Z}}'\big|_{t=t_0}$ are evaluated by means of the transformation

272 formula of the loading rates, which in view of Eq. (10) reads

273
$$L_\alpha'\Big|_{t=t_0} = (\frac{\partial F_\alpha'}{\partial \mathbf{E}'} : \dot{\mathbf{E}}' + \frac{\partial F_\alpha}{\partial \mathrm{T}'}\dot{\mathrm{T}}')\Big|_{t=t_0} =$$
$$= \frac{\partial F_\alpha}{\partial \mathbf{E}} : \dot{\mathbf{E}} + \frac{\partial F_\alpha}{\partial \mathbf{E}} : (\mathbf{w} \circ \bar{\mathbf{E}}) + \frac{\partial F_\alpha}{\partial \mathrm{T}}\dot{\mathrm{T}} + \frac{\partial F_\alpha}{\partial \mathrm{T}}(u\mathrm{T}).$$

274 Accordingly, the rate $\dot{\mathbf{E}}'_{\mathbf{Tr}}\big|_{t=t_0}$ is evaluated as

275
$$\dot{\mathbf{E}}'_{\mathbf{Tr}}\Big|_{t=t_0} = \sum_{\alpha=1}^{n} H_\alpha' \mathbf{L}_\alpha'(\mathbf{E}',\mathrm{T}',\mathbf{E}'_{\mathbf{Tr}},\mathbf{Z}')L_\alpha'\Big|_{t=t_0} =$$
$$= \sum_{\alpha=1}^{n} H_\alpha \mathbf{L}_\alpha(\mathbf{E},\mathrm{T},\mathbf{E}_{\mathbf{Tr}},\mathbf{Z})L_\alpha + \sum_{\alpha=1}^{n} H_\alpha \mathbf{L}_\alpha(\mathbf{E},\mathrm{T},\mathbf{E}_{\mathbf{Tr}},\mathbf{Z})[\frac{\partial F_\alpha}{\partial \mathbf{E}} : (\mathbf{w} \circ \bar{\mathbf{E}}) + \frac{\partial F_\alpha}{\partial \mathrm{T}}(u\,\mathrm{T})] =$$
$$= \dot{\mathbf{E}}_{\mathbf{Tr}} + \sum_{\alpha=1}^{n} H_\alpha \mathbf{L}_\alpha(\mathbf{E},\mathrm{T},\mathbf{E}_{\mathbf{Tr}},\mathbf{Z})[\frac{\partial F_\alpha}{\partial \mathbf{E}} : (\mathbf{w} \circ \bar{\mathbf{E}}) + \frac{\partial F_\alpha}{\partial \mathrm{T}}(u\,\mathrm{T})].$$

276 In a similar manner for $\dot{\mathbf{Z}}'\big|_{t=t_0}$ we derive

277
$$\dot{\mathbf{Z}}'\Big|_{t=t_0} = \dot{\mathbf{Z}} + \sum_{\alpha=1}^{n} H_\alpha \mathbf{M}_\alpha(\mathbf{E},\mathrm{T},\mathbf{E}_{\mathbf{Tr}},\mathbf{Z})[(\frac{\partial F_\alpha}{\partial \mathbf{E}} : (\mathbf{w} \circ \mathbf{E}) + \frac{\partial F_\alpha}{\partial \mathrm{T}}(u\mathrm{T})],$$

278 so that the transformed Helmholtz free energy reads

279
$$\dot{\Psi}'\Big|_{t=t_0} = \dot{\Psi} + \frac{\partial \Psi}{\partial \mathbf{E}} : (\mathbf{w} \circ \mathbf{E}) + \frac{\partial \Psi}{\partial \mathrm{T}} : (u\mathrm{T}) +$$
$$+ \frac{\partial \Psi}{\partial \mathbf{E}_{\mathbf{Tr}}} : \sum_{\alpha=1}^{n} H_\alpha \mathbf{L}_\alpha(\mathbf{E},\mathrm{T},\mathbf{E}_{\mathbf{Tr}},\mathbf{Z})[\frac{\partial F_\alpha}{\partial \mathbf{E}} : (\mathbf{w} \circ \bar{\mathbf{E}}) + \frac{\partial F_\alpha}{\partial \mathrm{T}}(u\mathrm{T})] + \tag{11}$$
$$+ \frac{\partial \Psi}{\partial \mathbf{Z}} : \sum_{\alpha=1}^{n} H_\alpha \mathbf{M}_\alpha(\mathbf{E},\mathrm{T},\mathbf{E}_{\mathbf{Tr}},\mathbf{Z})[\frac{\partial F_\alpha}{\partial \mathbf{E}} : (\mathbf{w} \circ \bar{\mathbf{E}}) + \frac{\partial F_\alpha}{\partial \mathrm{T}}(u\mathrm{T})].$$

280 Furthermore,

281
$$\mathbf{S}':\dot{\mathbf{E}}'\Big|_{t=t_0} = \mathbf{S}:\dot{\mathbf{E}}+\mathbf{S}:(\mathbf{w}\circ\mathbf{E}),\qquad(12)$$

282   In light of Eqs. (9), (11) and (12) the transformed balance of energy equation (at $t=t_0$)

283   can be written as

284
$$\rho_{ref}\{\dot{\Psi}+\frac{\partial\Psi}{\partial\mathbf{E}}:(\mathbf{w}\circ\mathbf{E})+\frac{\partial\Psi}{\partial\mathrm{T}}:(u\mathrm{T})+$$
$$\frac{\partial\Psi}{\partial\mathbf{E_{Tr}}}:\sum_{\alpha=1}^{n}H_{\alpha}\mathbf{L}_{\alpha}(\mathbf{E},\mathrm{T},\mathbf{E_{Tr}},\mathbf{Z})[\frac{\partial F_{\alpha}}{\partial\mathbf{E}}:(\mathbf{w}\circ\mathbf{E})+\frac{\partial F_{\alpha}}{\partial\mathrm{T}}(u\mathrm{T})]+$$
$$\frac{\partial\Psi}{\partial\mathbf{Z}}:\sum_{\alpha=1}^{n}H_{\alpha}\mathbf{M}_{\alpha}(\mathbf{E},\mathrm{T},\mathbf{E_{Tr}},\mathbf{Z})[\frac{\partial F_{\alpha}}{\partial\mathbf{E}}:(\mathbf{w}\circ\mathbf{E})+\frac{\partial F_{\alpha}}{\partial\mathrm{T}}(u\mathrm{T})]\}+\rho_{ref}N\dot{\mathrm{T}}+\rho_{ref}N(u\mathrm{T})+DIV\mathbf{H}=$$
$$\mathbf{S}:\dot{\mathbf{E}}+\mathbf{S}:(\mathbf{w}\circ\mathbf{E})+\rho_{ref}(R-\mathrm{T}\dot{N}).$$

285   (13)

286   By subtracting Eq. (6) from Eq. (13) and by involving the transformation formulae for the

287   heat flux vector and the apparent heat supply (recall Axiom 3) we can derive the following

288   identity

289
$$\rho_{ref}\frac{\partial\Psi}{\partial\mathbf{E}}:(\mathbf{w}\circ\bar{\mathbf{E}})+\rho_{ref}\frac{\partial\Psi'}{\partial\mathrm{T}}(u\mathrm{T})+$$
$$+\rho_{ref}[\frac{\partial\Psi}{\partial\mathbf{E_{Tr}}}:\sum_{\alpha=1}^{n}H_{\alpha}\mathbf{L}_{\alpha}(\mathbf{E},\mathrm{T},\mathbf{E_{Tr}},\mathbf{Z})\frac{\partial F_{\alpha}}{\partial\mathbf{E}}+\frac{\partial\Psi}{\partial\mathbf{Z}}:\sum_{\alpha=1}^{n}H_{\alpha}\mathbf{M}_{\alpha}(\mathbf{E},\mathrm{T},\mathbf{E_{Tr}},\mathbf{Z})\frac{\partial F_{\alpha}}{\partial\mathbf{E}}](\mathbf{w}\circ\bar{\mathbf{E}})+$$
$$+\rho_{ref}[\frac{\partial\Psi}{\partial\mathbf{E_{Tr}}}:\sum_{\alpha=1}^{n}H_{\alpha}\mathbf{L}_{\alpha}(\mathbf{E},\mathrm{T},\mathbf{E_{Tr}},\mathbf{Z})\frac{\partial F_{\alpha}}{\partial\mathrm{T}}+\frac{\partial\Psi}{\partial\mathbf{Z}}:\sum_{\alpha=1}^{n}H_{\alpha}\mathbf{M}_{\alpha}(\mathbf{E},\mathrm{T},\mathbf{E_{Tr}},\mathbf{Z})\frac{\partial F_{\alpha}}{\partial\mathrm{T}}](u\mathrm{T})+$$
$$+\rho_{ref}N(u\mathrm{T})-\mathbf{S}:(\mathbf{w}\circ\bar{\mathbf{E}})=0,$$

290   or equivalently

291
$$\{\rho_{ref}[\frac{\partial\Psi}{\partial\mathbf{E}}+\frac{\partial\Psi}{\partial\mathbf{E_{Tr}}}:\sum_{\alpha=1}^{n}H_{\alpha}\mathbf{L}_{\alpha}(\mathbf{E},\mathrm{T},\mathbf{E_{Tr}},\mathbf{Z})\frac{\partial F_{\alpha}}{\partial\mathbf{E}}+$$
$$+\frac{\partial\Psi}{\partial\mathbf{Z}}:\sum_{\alpha=1}^{n}H_{\alpha}\mathbf{M}_{\alpha}(\mathbf{E},\mathrm{T},\mathbf{E_{Tr}},\mathbf{Z})\frac{\partial F_{\alpha}}{\partial\mathbf{E}}]-\mathbf{S}\}:(\mathbf{w}\circ\mathbf{E})\}+$$
$$+\rho_{ref}[\frac{\partial\Psi}{\partial\mathrm{T}}+\frac{\partial\Psi}{\partial\mathbf{E_{Tr}}}:\sum_{\alpha=1}^{n}H_{\alpha}\mathbf{L}_{\alpha}(\mathbf{E},\mathrm{T},\mathbf{E_{Tr}},\mathbf{Z})\frac{\partial F_{\alpha}}{\partial\mathrm{T}}+$$
$$+\frac{\partial\Psi}{\partial\mathbf{Z}}:\sum_{\alpha=1}^{n}H_{\alpha}\mathbf{M}_{\alpha}(\mathbf{E},\mathrm{T},\mathbf{E_{Tr}},\mathbf{Z})\frac{\partial F_{\alpha}}{\partial\mathrm{T}}+N](u\mathrm{T})=0.$$

(14)

292 from which by noting that $\mathbf{w}$ and u can be arbitrarily specified, we can derive

$$\mathbf{S} = \rho_{ref}[\frac{\partial \Psi}{\partial \mathbf{E}} + \frac{\partial \Psi}{\partial \mathbf{E_{Tr}}} : \sum_{\alpha=1}^{n} H_\alpha \mathbf{L}_\alpha(\mathbf{E}, T, \mathbf{E_{Tr}}, \mathbf{Z})\frac{\partial F_\alpha}{\partial \mathbf{E}} +$$

$$\frac{\partial \Psi}{\partial \mathbf{Z}} : \sum_{\alpha=1}^{n} H_\alpha \mathbf{M}_\alpha(\mathbf{E}, T, \mathbf{E_{Tr}}, \mathbf{Z})\frac{\partial F_\alpha}{\partial \mathbf{E}}],$$

293 $\qquad\qquad\qquad\qquad\qquad\qquad\qquad\qquad\qquad\qquad\qquad$ (15)

$$N = -[\frac{\partial \Psi}{\partial T} + \frac{\partial \Psi}{\partial \mathbf{E_{Tr}}} : \sum_{\alpha=1}^{n} H_\alpha \mathbf{L}_\alpha(\mathbf{E}, T, \mathbf{E_{Tr}}, \mathbf{Z})\frac{\partial F_\alpha}{\partial T} +$$

$$+\frac{\partial \Psi}{\partial \mathbf{Z}} : \sum_{\alpha=1}^{n} H_\alpha \mathbf{M}_\alpha(\mathbf{E}, T, \mathbf{E_{Tr}}, \mathbf{Z})\frac{\partial F_\alpha}{\partial T}].$$

294 i.e., unlike the classical elastic case discussed in Marsden and Hughes [23, pp. 202-203],

295 for the material undergoing phase transformations, the covariance of the local form of the

296 energy balance, *does not yield the standard thermomechanical relations*

297 $$\mathbf{S} = \rho_{ref}\frac{\partial \Psi}{\partial \mathbf{E}}, \quad N = -\frac{\partial \Psi}{\partial T},$$ $\qquad\qquad$ (16)

298 *unless a further assumption is made*, namely that there exists a spatial diffeomorphism

299 (ξ, δ) which results in an unloading process from an inelastic state (i.e. a process with

300 $J_{adm} \neq \varnothing$ and $J_{act} = \varnothing$) which is *quasi-reversible* (see Fosdick and Serrinin [11]). This

301 means that in such a process the inelastic (transformation) work W_{in}, defined as

$$W_{in} = \rho_{ref}[\frac{\partial \Psi}{\partial \mathbf{E_{Tr}}} : \sum_{\alpha=1}^{n} H_\alpha \mathbf{L}_\alpha(\mathbf{E}, T, \mathbf{E_{Tr}}, \mathbf{Z})\frac{\partial F_\alpha}{\partial \mathbf{E}} +$$

$$\frac{\partial \Psi}{\partial \mathbf{Z}} : \sum_{\alpha=1}^{n} H_\alpha \mathbf{M}_\alpha(\mathbf{E}, T, \mathbf{E_{Tr}}, \mathbf{Z})\frac{\partial F_\alpha}{\partial \mathbf{E}}] : (\mathbf{w} \circ \mathbf{E}) -$$

302

$$-[\frac{\partial \Psi}{\partial \mathbf{E_{Tr}}} : \sum_{\alpha=1}^{n} H_\alpha \mathbf{L}_\alpha(\mathbf{E}, T, \mathbf{E_{Tr}}, \mathbf{Z})\frac{\partial F_\alpha}{\partial T} +$$

$$+\frac{\partial \Psi}{\partial \mathbf{Z}} : \sum_{\alpha=1}^{n} H_\alpha \mathbf{M}_\alpha(\mathbf{E}, T, \mathbf{E_{Tr}}, \mathbf{Z})\frac{\partial F_\alpha}{\partial T}](uT)$$

303   *that is, the work performed by the internal variables during the action of (ξ, δ) vanishes.*

304   Then, in this case the standard thermomechanical relations follow directly from Eq. (14)

305   for $W_{\mathbf{in}} = 0$. It is noted that the expressions

306

$$W_{\mathbf{in}mech} = -\rho_{ref}[\frac{\partial \Psi}{\partial \mathbf{E_{Tr}}} : \sum_{\alpha=1}^{n} H_\alpha \mathbf{L}_\alpha (\mathbf{E}, \mathrm{T}, \mathbf{E_{Tr}}, \mathbf{Z}) \frac{\partial F_\alpha}{\partial \mathbf{E}} +$$

$$+ \frac{\partial \Psi}{\partial \mathbf{Z}} : \sum_{\alpha=1}^{n} H_\alpha \mathbf{M}_\alpha (\mathbf{E}, \mathrm{T}, \mathbf{E_{Tr}}, \mathbf{Z}) \frac{\partial F_\alpha}{\partial \mathbf{E}}] : (\mathbf{w_t} \circ \mathbf{E}),$$

$$W_{\mathbf{in}thermal} = [\frac{\partial \Psi}{\partial \mathbf{E_{Tr}}} : \sum_{\alpha=1}^{n} H_\alpha \mathbf{L}_\alpha (\mathbf{E}, \mathrm{T}, \mathbf{E_{Tr}}, \mathbf{Z}) \frac{\partial F_\alpha}{\partial \mathrm{T}} +$$

$$+ \frac{\partial \Psi}{\partial \mathbf{Z}} : \sum_{\alpha=1}^{n} H_\alpha \mathbf{M}_\alpha (\mathbf{E}, \mathrm{T}, \mathbf{E_{Tr}}, \mathbf{Z}) \frac{\partial F_\alpha}{\partial \mathrm{T}}] (u_\mathbf{t} \mathrm{T}),$$

307   stand for the mechanical and thermal work produced by the superposed spatial

308   diffeomorphism and the temperature rescaling, respectively.

309   Note that the result derived herein is in absolute accordance with the one derived on the

310   basis of the second law of thermodynamics by Lubliner and Auricchio in [22]. More

311   information on this point is provided by Panoskaltsis in [32].

312

313   **REMARK 1**   The concept of the covariant energy balance has been also exploited by

314   Panoskaltsis in [32], but unlike the present case where we consider the covariance of the

315   referential balance of energy equation, Panoskaltsis considers *covariance of the spatial*

316   *energy balance*. Contrary to the present formulation, Panoskaltsis in [32] derives the stress-

317   strain relations in a spatial setting in terms of the Cauchy stress tensor $\boldsymbol{\sigma}$ and the Almansi

318   strain $\mathbf{e}$. More specifically, Panoskaltsis in [32] derives the standard stress-strain relations

319

$$\boldsymbol{\sigma} = \rho \frac{\partial \psi}{\partial \mathbf{e}},$$

320   where ρ and ψ stand for the mass density and the Helmholtz free energy in the spatial

321   configuration.

322

323   ***REMARK 2*** Eqs. (15) constitute the *covariance conditions* for the energy balance equation

324   (6) i.e. the necessary conditions, so that this equation is *invariant* under the superposition

325   of arbitrary diffeomorphisms acting on the Euclidean space, *DiffS*, which include also a

326   temperature rescaling $\delta \in R^+$. Moreover, it can be proved that the conditions (15) are also

327   sufficient. This means *that if we do not consider the assumption related to the existence of*

328   *quasi-reversible processes*, the invariance (symmetry) group of the balance of energy

329   equation is

$$G = \{(\boldsymbol{\xi},\delta) \in DiffS \times R^+ \ /$$

$$\mathbf{S} = \rho_{ref}[\frac{\partial \Psi}{\partial \mathbf{E}} + \frac{\partial \Psi}{\partial \mathbf{E_{Tr}}} : \sum_{\alpha=1}^{n} H_\alpha \mathbf{L}_\alpha(\mathbf{E}, T, \mathbf{E_{Tr}}, \mathbf{Z}) \frac{\partial F_\alpha}{\partial \mathbf{E}} +$$

330
$$\frac{\partial \Psi}{\partial \mathbf{Z}} : \sum_{\alpha=1}^{n} H_\alpha \mathbf{M}_\alpha(\mathbf{E}, T, \mathbf{E_{Tr}}, \mathbf{Z}) \frac{\partial F_\alpha}{\partial \mathbf{E}}] \text{ and}$$

$$N = -[\frac{\partial \Psi}{\partial T} + \frac{\partial \Psi}{\partial \mathbf{E_{Tr}}} : \sum_{\alpha=1}^{n} H_\alpha \mathbf{L}_\alpha(\mathbf{E}, T, \mathbf{E_{Tr}}, \mathbf{Z}) \frac{\partial F_\alpha}{\partial T} +$$

$$+ \frac{\partial \Psi}{\partial \mathbf{Z}} : \sum_{\alpha=1}^{n} H_\alpha \mathbf{M}_\alpha(\mathbf{E}, T, \mathbf{E_{Tr}}, \mathbf{Z}) \frac{\partial F_\alpha}{\partial T}]\}.$$

331   In this case it can be proved - see Panoskaltsis and Soldatos in [35] - that *the material*

332   *response is elastic (non-dissipative)*. Upon the *consideration of elastic-inelastic response*,

333   *the covariance group G is restricted to* the group

$$G' = \{(\boldsymbol{\xi},\delta) \in DiffS \times R^+ \ /\mathbf{S} = \rho_{ref} \frac{\partial \Psi}{\partial \mathbf{E}}, \ N = -\frac{\partial \Psi}{\partial T}, \ W_{in\,mech} = 0 \text{ and } W_{in\,hermal} = 0\},$$

335   In this sense, the present approach and its basic conclusions are consistent with the modern

336   approach to symmetries in physics, as emphasized for instance by Earman [10]:

18

337   • *The symmetries are in the laws of the phenomena, not in the phenomena*

338   *themselves*

339   • *The phenomena break the symmetries of laws.*

340

341 **REMARK 3** An alternative approach to the concept of invariance could be provided by noting

342 the natural connection which exists between conservation laws and the symmetries of the

343 (dynamical) system in question. In particular, if the Euler-Lagrange equations of the system

344 are satisfied and the Lagrangian is invariant under the action of some group of

345 transformations, Noether's theorem establishes the existence and the precise nature of the

346 corresponding conserved quantities. Such an approach has been favored, among others by

347 Rahuadjet al.[41, 42] and Romero [46] (see also [12, 53]).

348

349

350   *2.3 The temperature evolution equation*

351

352 As a final step we derive a general equation for the temperature evolution which occurs in

353 the course of phase transformations. This is done on the basis of the energy balance

354 equation (recall Eq. (6)). In this case, the time derivative of the Helmholtz free energy

355 yields

356
$$\rho_{\text{ref}}\left(\frac{\partial \Psi}{\partial \mathbf{E}}:\dot{\mathbf{E}}+\frac{\partial \Psi}{\partial \mathbf{E_{Tr}}}:\dot{\mathbf{E}}_{\mathbf{Tr}}+\frac{\partial \Psi}{\partial \mathbf{Z}}\dot{\mathbf{Z}}+\frac{\partial \Psi}{\partial \mathrm{T}}\dot{\mathrm{T}}\right)+\rho_{\text{ref}}N\dot{\mathrm{T}}+\rho_{\text{ref}}\dot{N}\mathrm{T}+DIV\mathbf{H}=\rho_{\text{ref}}\mathrm{R}+\mathbf{S}{:}\dot{\mathbf{E}}, \quad (17)$$

357 which in turn upon substitution of the thermomechanical state Eqs. (16) yields

358
$$\rho_{\text{ref}}\left(\frac{\partial \Psi}{\partial \mathbf{E^{Tr}}}:\dot{\mathbf{E}}_{\mathbf{Tr}}+\frac{\partial \Psi}{\partial \mathbf{Z}}:\dot{\mathbf{Z}}\right)+\rho_{\text{ref}}\dot{N}\mathrm{T}+DIV\mathbf{H}=\rho_{\text{ref}}\mathrm{R}. \quad (18)$$

19

359 The time derivative of the entropy density is determined by the second of Eqs. (16) as

$$\dot{N} = -\frac{\partial^2 \Psi}{\partial T \partial \mathbf{E}} : \dot{\mathbf{E}} - \frac{\partial^2 \Psi}{\partial T \partial \mathbf{E}_{\mathbf{Tr}}} : \dot{\mathbf{E}}_{\mathbf{Tr}} - \frac{\partial^2 \Psi}{\partial T \partial \mathbf{Z}} : \dot{\mathbf{Z}} - \frac{\partial^2 \Psi}{\partial T^2} \dot{T}, \qquad (19)$$

361 which upon defining the specific heat c at constant deformation and internal variables as

$$c = -\frac{\partial^2 \Psi}{\partial T^2} T, \qquad (20)$$

363 and upon substitution of Eqs. (19) and (20), reads

$$c\dot{T} = -(\frac{\partial \Psi}{\partial \mathbf{E}_{\mathbf{Tr}}} : \dot{\mathbf{E}}_{\mathbf{Tr}} + \frac{\partial \Psi}{\partial \mathbf{Z}} : \dot{\mathbf{Z}}) + (\frac{\partial^2 \Psi}{\partial T \partial \mathbf{E}} : \dot{\mathbf{E}} + \frac{\partial^2 \Psi}{\partial T \partial \mathbf{E}_{\mathbf{Tr}}} : \dot{\mathbf{E}}_{\mathbf{Tr}} + \frac{\partial^2 \Psi}{\partial T \partial \mathbf{Z}} : \dot{\mathbf{Z}})T + (R - \frac{1}{\rho_{\mathrm{ref}}} D\!I\!V\mathbf{H}),$$

365 which constitutes the temperature evolution equation in a non-isothermal process. This

366 equation upon defining the *elastic contribution to heating* as

$$\dot{Q}_{\mathrm{e}} = T(\frac{\partial^2 \Psi}{\partial T \partial \mathbf{E}} : \dot{\mathbf{E}} + \frac{\partial^2 \Psi}{\partial T \partial \mathbf{E}_{\mathbf{Tr}}} : \dot{\mathbf{E}}_{\mathbf{Tr}}) = T[\frac{\partial^2 \Psi}{\partial T \partial \mathbf{E}} : (\dot{\mathbf{E}} - \dot{\mathbf{E}}^{\mathrm{Tr}})]$$

$$T[\frac{\partial^2 \Psi}{\partial (\mathbf{E} - \mathbf{E}_{\mathbf{Tr}})\partial T} : (\dot{\mathbf{E}} - \dot{\mathbf{E}}_{\mathbf{Tr}})] = T\frac{\partial^2 \Psi}{\partial \mathbf{E}_{\mathrm{e}}\partial T} : \dot{\mathbf{E}}_{\mathrm{e}},$$

368 and the *inelastic (transformation)* one as

$$\dot{Q}_{\mathrm{Tr}} = -(\frac{\partial \Psi}{\partial \mathbf{E}_{\mathbf{Tr}}} : \dot{\mathbf{E}}_{\mathbf{Tr}} + \frac{\partial \Psi}{\partial \mathbf{Z}} : \dot{\mathbf{Z}}) + T\frac{\partial^2 \Psi}{\partial T \partial \mathbf{Z}} : \dot{\mathbf{Z}},$$

370 takes the following remarkably simple form (see Rosakis et al. in [47])

$$c\dot{T} = \dot{Q}_{\mathrm{e}} + \dot{Q}_{\mathrm{Tr}} + (R - \frac{1}{\rho_{\mathrm{ref}}} DIV\mathbf{H}). \qquad (21)$$

372 which has the obvious advantage of decoupling the elastic and inelastic contributions to

373 material heating and is well suited for computational use.

374

375 **REMARK 4** Upon defining, the inelastic dissipation D as

376

$$D = -(\frac{\partial \Psi}{\partial \mathbf{E}_{\mathbf{Tr}}} : \dot{\mathbf{E}}_{\mathrm{Tr}} + \frac{\partial \Psi}{\partial \mathbf{Z}} : \dot{\mathbf{Z}}),$$

377   and the elastic-inelastic structural heating H as

378

$$H = -\mathrm{T}\frac{\partial}{\partial \mathrm{T}}(\mathbf{S} : \dot{\mathbf{E}} - D),$$

379   the temperature evolution equation takes the alternative form

380

$$c\dot{\mathrm{T}} = (D - H) + (-\frac{1}{\rho_{\mathrm{ref}}}DIV\mathbf{H} + \mathrm{R}). \tag{22}$$

381   In this equation H is associated to the non-dissipative (latent) elastic-plastic changes due

382   to thermal phenomena. This term as it will be clear in the foregoing - see Section 4.3.1 -

383   plays a very important role in thermo-mechanically coupled problems in SMAs.

384

385   **REMARK 5** An equivalent equation for the temperature evolution equation can be also

386   derived in the spatial configuration by either working in a similar manner in terms of the

387   spatial variables or by means of a push-forward operation to Eq. (22). The resulting

388   expression in is

389

$$c\dot{\mathrm{T}} = (d - h) + (-\frac{1}{\rho}div\mathbf{h} + r), \tag{23}$$

390   where

391

$$d = -(\frac{\partial \psi}{\partial \mathbf{e}_{\mathbf{Tr}}} : L_v\mathbf{e}_{\mathbf{Tr}} + \frac{\partial \Psi}{\partial \mathbf{z}} : \dot{\mathbf{z}}), \quad h = -\mathrm{T}\frac{\partial}{\partial \mathrm{T}}(\boldsymbol{\tau} : L_v\mathbf{e} - d). \tag{23}$$

392   are the expressions for the plastic dissipation d and the structural heating structural h

393   "as seen" in the spatial configuration. Further, in Eq. (23), $\psi = \psi(\mathbf{e}, \mathrm{T}, \mathbf{e}_{\mathbf{Tr}}, \mathbf{z})$ is the

394   Helmholtz free energy in terms of the spatial variables, while ρ, $div(\cdot)$, $\mathbf{h}$ and r, stand

395   for the mass density, the divergence operator, the heat flux vector and the heat supply

21

396   in the spatial configuration. Such a form of the temperature evolution equation has been

397   favored by Simo and Miehe [48] and may be implemented in cases where a spatial

398   formulation of a material model is simpler than the material one (see e.g. Panoskaltsis

399   et al. in [39]).

400

401

402   **3   A model problem**

403

404   In the preceding Sections, the proposed formulation is presented largely in an abstract

405   manner by leaving the number and the nature of the internal variables, underlying the phase

406   transformations, unspecified. To clarify the application of generalized plasticity within a

407   thermomechanical modelling setting for phase transformations, a material model is

408   presented in this Section.

409   Without loss of generality, we confine our attention to phase transformations between the

410   austenite and a single (favorably) oriented martensite variant. The internal variable vector

411   **Z**, as it is common with this class of the models for SMAs (see, e.g., [43, 8, 22, 29, 33, 38,

412   52]) is assumed to be composed by a single scalar internal variable - say ξ -the phase

413   fraction of martensite within the continuum. The (forward)austenite to martensite

414   transformation will be denoted symbolically as the (M) transformation, while the (reverse)

415   martensite to austenite transformation will be denoted as the (A) one.

416   In view of the additive decomposition of the strain tensor (2), the Helmholtz free energy

417   can be additively decomposed in a part Ψ_e which corresponds to elastic and thermal

418   expansion behavior and an inelastic (due to phase transformations) part Ψ_{Tr}, as follows

22

419
$$\rho_{ref}\Psi = \rho_{ref}\Psi_{\mathbf{e}}(\mathbf{E} - \mathbf{E}_{\mathbf{Tr}}(\xi), \mathrm{T}, \xi) + \rho_{ref}\Psi_{\mathbf{Tr}}(\xi, \mathrm{T}). \tag{24}$$

420   It is emphasized that this is not the conventional decomposition of the free energy function

421   performed within the classical inelastic theories (e.g. plasticity, viscoelasticity,

422   viscoplasticity), since the elastic part $\Psi_{\mathbf{e}}$ depends on the internal variable ξ. In this sense

423   the decomposition (24) resembles the decompositions employed within the

424   thermomechanical treatment of damage (see [33]). The elastic part of the Helmholtz free

425   energy, under the valid assumption that elastic thermal effects are negligible in comparison

426   to transformation induced thermal effects, may be assumed to be given by the expression

427   of the stored energy function of a St. Venant-Kirchhoff material (see, e.g., [23, pp. 223,

428   225]; [13, pp. 250-251]), that is

429   $$\Psi_{\mathbf{e}}(\mathbf{E} - \mathbf{E}_{\mathbf{Tr}}(\xi), \mathrm{T}) = \Psi_{\mathbf{e}}(\mathbf{E} - \mathbf{E}_{\mathbf{Tr}}(\xi)) = \frac{\lambda(\xi)}{2}\{tr[\mathbf{E} - \mathbf{E}_{\mathbf{Tr}}(\xi)\}^2 + \mu(\xi)tr[(\mathbf{E} - \mathbf{E}_{\mathbf{Tr}}(\xi)]^2,$$

430   where λ and μ are the Lame′ parameters ($\lambda > 0$, $\mu > 0$), which are defined in terms of the

431   standard elastic constants E, ν as

432   $$\lambda = \frac{\nu E}{(1+\nu)(1-2\nu)}, \quad \mu = \frac{E}{2(1+\nu)}.$$

433   These are assumed to be dependent on the martensite fraction of the SMA, according to

434   the standard law of mixtures

435   $$\lambda(\xi) = \lambda_{\mathbf{A}} + \xi(\lambda_{\mathbf{M}} - \lambda_{\mathbf{A}}), \quad \mu(\xi) = \mu_{\mathbf{A}} + \xi(\mu_{\mathbf{M}} - \mu_{\mathbf{A}}),$$

436   where $\lambda_{\mathbf{A}}$, $\mu_{\mathbf{A}}$ are the Lame′ parameters when the material is fully austenite, and $\lambda_{\mathbf{M}}$, $\mu_{\mathbf{M}}$

437   are these when the material is fully martensite. For the transformation part of the Helmholtz

438   free energy, by following Raniecki et al. in [42] - see also [44], [29] - we consider an

439   expression of the form

440
$$\Psi_{\mathbf{Tr}} = (1-\xi)\Psi_{\mathbf{Chem}}^{\mathbf{A}} + \xi\Psi_{\mathbf{Chem}}^{\mathbf{M}} + \Delta^{\mathbf{AM}}\Psi,$$

441 where $\Psi_{\mathbf{Chem}}^{\mathbf{A}}$ and $\Psi_{\mathbf{Chem}}^{\mathbf{M}}$ are the chemical energies of the austenite and martensite phases

442 respectively, and $\Delta^{\mathbf{AM}}\Psi$ results from the interaction between these phases. For these

443 energies we assume the following expressions (see also [29])

$$\Psi_{\mathbf{Chem}}^{\mathbf{A}} = (u_0^{*\mathbf{A}} - Ts_0^{*\mathbf{A}}) + c[(T-T_0) - T\ln\left(\frac{T}{T_0}\right)]$$

444
$$\Psi_{\mathbf{Chem}}^{\mathbf{M}} = (u_0^{*\mathbf{M}} - Ts_0^{*\mathbf{M}}) + c[(T-T_0) - T\ln\left(\frac{T}{T_0}\right)],$$

$$\Delta^{\mathbf{AM}}\Psi = Z(1-Z)(\bar{u}_0 - T\bar{s}_0),$$

445 where T_0 is the reference temperature and $u_0^{*\mathbf{A}}$, $s_0^{*\mathbf{A}}$, $u_0^{*\mathbf{M}}$, $s_0^{*\mathbf{M}}$, $\bar{u}_0$ and $\bar{s}_0$ are the thermal

446 parameters of the model.

447   Then in light of the first of Eqs. (16) the second Piola-Kirchhoff stress tensor is found to

448 be

449
$$\mathbf{S} = \lambda tr(\mathbf{E} - \mathbf{E}_{\mathbf{Tr}})\mathbf{1} + 2\mu(\mathbf{E} - \mathbf{E}_{\mathbf{Tr}}), \tag{25}$$

450 where $\mathbf{1}$ is the unit rank-2 tensor, and the dependence of the involved quantities on ξ has

451 been dropped for convenience.

452   As in Panoskaltsis et al. [36], the loading surfaces are assumed to be given in the stress-

453 space as a two parameter family of von-Mises type surfaces, that is

454
$$F(\mathbf{S},T) = |DEV\mathbf{S}| - CT - R = 0, \tag{26}$$

455 where $|\cdot|$ stands for the Euclidean norm, $DEV(\cdot)$ stands for the deviatoric part of the stress

456 tensor in the reference configuration and C R are the family parameters. On substituting

457 from Eq. (25) into equation (26) the equivalent expression for the loading surfaces in strain-

458 space may be derived as

459 $$F(\mathbf{E},\mathbf{E_{Tr}},T) = 2\mu\,\left|DEV(\mathbf{E}-\mathbf{E_{Tr}})\right| - CT - R = 0.$$

460 For the rate equation for the evolution of the transformation strain we assume a normality

461 rule in the strain-space which is given as

462 $$2\mu\dot{\mathbf{E}}_{\mathbf{Tr}} = \sqrt{\frac{3}{2}}\varepsilon_{\mathbf{L}}\dot{\xi}\frac{\partial F}{\partial \mathbf{E}}, \tag{27}$$

463 where $\varepsilon_{\mathbf{L}}$ is a material constant, which is defined as the maximum inelastic strain (see, e.g.,

464 [7,22]), which is attained in the case of one-dimensional unloading in simple tension when

465 the material is fully martensite.

466 In order to close the model, as in our previous work in [36] - see also Auricchio et al. [5]

467 -, we consider a linear expression for the evolution of ξ, which within the present

468 formulation can be expressed as

469 $$\dot{\xi} = -\frac{\langle -F_{\mathbf{Mf}}F_{\mathbf{Ms}}\rangle}{\left|F_{\mathbf{Mf}}F_{\mathbf{Ms}}\right|}\frac{\langle M_{\mathbf{d}}-T\rangle}{\left|T-M_{\mathbf{d}}\right|}\frac{1-\xi}{F_{\mathbf{Mf}}-2\mu\varepsilon_{\mathbf{L}}(1-\xi)}\langle L_{\mathbf{M}}\rangle - \frac{\langle -F_{\mathbf{Af}}F_{\mathbf{As}}\rangle}{\left|F_{\mathbf{Af}}F_{\mathbf{As}}\right|}\frac{\xi}{F_{\mathbf{Af}}+2\mu\varepsilon_{\mathbf{L}}\xi}\langle L_{\mathbf{A}}\rangle,$$

470 $$\tag{28}$$

471 where

472 $$F_{\mathbf{Mf}}(\mathbf{E},\mathbf{E_{Tr}},T) = 2\mu\,\left|DEV(\mathbf{E}-\mathbf{E_{Tr}})\right| - \sqrt{\frac{2}{3}}C_{\mathbf{M}}(T-M_{\mathbf{f}}),$$

473 $$F_{\mathbf{Ms}}(\mathbf{E},\mathbf{E_{Tr}},T) = 2\mu\,\left|DEV(\mathbf{E}-\mathbf{E_{Tr}})\right| - \sqrt{\frac{2}{3}}C_{\mathbf{M}}(T-M_{\mathbf{s}}),$$

474 $$F_{\mathbf{As}}(\mathbf{E},\mathbf{E_{Tr}},T) = 2\mu\,\left|DEV(\mathbf{E}-\mathbf{E_{Tr}})\right| - \sqrt{\frac{2}{3}}C_{\mathbf{A}}(T-A_{\mathbf{s}}),$$

475 $$F_{\mathbf{Af}}(\mathbf{E},\mathbf{E_{Tr}},T) = 2\mu\,\left|DEV(\mathbf{E}-\mathbf{E_{Tr}})\right| - \sqrt{\frac{2}{3}}C_{\mathbf{A}}(T-A_{\mathbf{f}}),$$

476 $$L_{\mathbf{M}} = -L_{\mathbf{A}} = \frac{\partial F}{\partial \mathbf{E}}:\dot{\mathbf{E}} + \frac{\partial F}{\partial T}\dot{T},$$

477 in which $C_\mathbf{M}$, $C_\mathbf{A}$, $M_\mathbf{f}$, $M_\mathbf{s}$, $A_\mathbf{s}$ and $A_\mathbf{f}$ are (standard) material parameters which can be

478 determined by means of the well-known (see, e.g., [22]) critical stress-temperature diagram

479 for the SMAs transformations; the geometrical interpretation of Eqs.

480 $F_\mathbf{Mf} = 0$, $F_\mathbf{Ms} = 0$, $F_\mathbf{As} = 0$ and $F_\mathbf{Af} = 0$ can be determined also by means of the

481 aforementioned critical diagram (see also [22]). Finally, $M_\mathbf{d}$ is a critical temperature value

482 above which the austenite is stable and the forward (M) transformation cannot be

483 activated (see McKelvey and Ritchie in [24]).

484 The formulation is supplemented by a constitutive law for the heat flux vector (see Eqs.

485 (21), (22)) which is assumed to be given by the standard Fourier's law (see, e.g., [48, 29])

486 as per

$$\mathbf{H} = -kGRAD\mathrm{T}, \tag{29}$$

488 where $GRAD(\cdot)$ is the gradient operator and k is the material conductivity.

489

490

491

492

493

494

495

496 **4 Numerical simulations**

497

498 In this Section we implement numerically the material model introduced in Section 3andwe

499 present a set of comprehensive numerical examples in order to show its ability in

500 simulating several patterns of the extremely complex behavior of SMAs under non-

501 isothermal conditions.

502 The numerical implementation of the proposed model can be performed by means of the

503 so-called *isothermal split*, suggested in the pioneering work of Simo and Miehe [48]. The

504 basic idea is to solve the governing equations of the coupled thermomechanical problem

505 (equations of motion, constitutive equations, energy balance equation and appropriate

506 boundary conditions) by performing *a natural split into a non-linear inelastic problem with*

507 *frozen thermal variables* (step 1), followed by *a heat conduction problem at fixed*

508 *configuration* (step 2). These two steps are coupled via the elastic $(\dot{Q}_{\mathrm{e}})$ and the inelastic

509 $(\dot{Q}_{\mathrm{Tr}})$ contributions to heating. The inelastic problem (step 1), can be pursued by means

510 of a predictor-corrector algorithm. Nevertheless, since the theory of plasticity employed

511 herein *is not a conventional one*, the proposed algorithmic scheme - see [33, 38] - differs

512 vastly from the standard return mapping algorithm employed within the context of classical

513 plasticity theories.

514

515 *4.1 Basic computational aspects*

516

517 The basic point for the numerical implementation of the model relies crucially on realizing

518 that when the deformation gradient **F** and the heat flux **H** are known at the material point

519 **X,** the rate equations for the evolution of the internal variables (Eqs. (27) and (28)), the

520 balance of energy equation (21) and the stress-strain relations (25), form, *at the local level*,

521 a system of four equations in the four unknowns **S**, T **E$_{\mathrm{Tr}}$** and ξ. Thus the implementation

522 problem is just reduced to the problem of solving numerically the aforementioned system.

523 The details of the solution procedure follow.

524 Let $J \in [0,T]$ be the time interval of interest. It is assumed that at time $t_n \in J$, the

525 configuration of the body of interest $\omega_n = x_n(\Omega)$, i.e. $x_n \equiv \{\mathbf{x}_n = \mathbf{x}_n(\mathbf{X}) / \mathbf{X} \in \Omega\}$, along

526 with the state variables

527 $$\{\mathbf{E}_n, \mathrm{T}_n, \mathbf{E}_{\mathrm{Trn}}, \xi_n, \mathbf{H}_n, \mathbf{S}_n\},$$

528 are known.

529 Assume a time increment Δt, which drives

530 • the time to t_{n+1},

531 • the body configuration to

532 $$x_{n+1} \equiv \{\mathbf{x}_{n+1} = \mathbf{x}_{n+1}(\mathbf{X}) / \mathbf{X} \in \Omega\},$$

533 where

534 $$\mathbf{x}_{n+1}(\mathbf{X}) = \mathbf{x}_n(\mathbf{X}) + \mathbf{u}(\mathbf{x}_n(\mathbf{X})),$$

535 and $\mathbf{u}$ is the given incremental displacement field,

536 • the temperature to T_{n+1}.

537 Then the algorithmic problem at hand is to update the internal variable vector $\begin{bmatrix} \mathbf{E}_{\mathrm{Tr}} \\ \xi \end{bmatrix}$, and

538 the stress tensor $\mathbf{S}$ to the time step t_{n+1} in a manner consistent with the (time continuous)

539 Eqs. (27), (28), (21) and (25). Note that the heat flux vector $\mathbf{H}_{n+1}$ is a function of the

540 temperature at time t_{n+1} defined by the Fourier's law (29). The solution of this problem is

541 pursued by a two-step algorithm - see further [48]-, which comprises an isothermal elastic-

542 inelastic problem followed by a heat conduction problem as follows

543

544   *Step 1: Isothermal elastic-inelastic problem*

545   As a first step we assume an isothermal problem $(\tilde{T}_{n+1} = T_n)$ defined at the configuration

546   x_{n+1}. The material strain tensor $\mathbf{E}_{n+1}$ is determined by means of the corresponding

547   deformation gradient $\mathbf{F}_{n+1}$ and the right Cauchy-Green tensor $\mathbf{C}_{n+1}$ as

548
$$\mathbf{F}_{n+1}(\mathbf{X}) = \mathbf{F}_{n+1} = \frac{\partial \mathbf{x}_{n+1}}{\partial \mathbf{X}}, \ \mathbf{C}_{n+1} = \mathbf{F}_{n+1}^{\mathrm{T}}\mathbf{F}_{n+1}, \ \mathbf{E}_{n+1} = \frac{1}{2}(\mathbf{C}_{n+1} - \mathbf{I}).$$

549   The application of the backward-Euler difference scheme for fixed temperature $\tilde{T}_{n+1}$ leads

550   to the following problem of evolution

551
$$2\mu(\tilde{\mathbf{E}}_{\mathrm{Tr}\,n+i} - \mathbf{E}_{\mathrm{Tr}\,n}) = \sqrt{\frac{3}{2}}\varepsilon_{\mathrm{L}}(\tilde{\xi}_{n+1} - \xi_n)\left(\frac{\partial \tilde{F}_{n+1}}{\partial \mathbf{E}}\right)_{n+1} \tag{30}$$

552
$$\tilde{\xi}_{n+1} - \xi_n = -\frac{\left\langle -\tilde{F}_{\mathrm{Mfn+1}}\tilde{F}_{\mathrm{Msn+1}}\right\rangle}{\left|\tilde{F}_{\mathrm{Mfn+1}}\tilde{F}_{\mathrm{Msn+1}}\right|}\frac{\left\langle M_{\mathrm{d}} - \tilde{T}_{n+1}\right\rangle}{\left|\tilde{T}_{n+1} - M_{\mathrm{d}}\right|}\frac{1 - \tilde{\xi}_{n+1}}{\tilde{F}_{\mathrm{Mn+1}} - 2\mu\varepsilon_{\mathrm{L}}(1 - \tilde{\xi}_{n+1})}\left\langle \tilde{L}_{\mathrm{Mn+1}}\right\rangle$$
$$- \frac{\left\langle -\tilde{F}_{\mathrm{Afn+1}}\tilde{F}_{\mathrm{Asn+1}}\right\rangle}{\left|\tilde{F}_{\mathrm{Afn+1}}\tilde{F}_{\mathrm{Asn+1}}\right|}\frac{\tilde{\xi}_{n+i}}{\tilde{F}_{\mathrm{Afn+1}} + 2\mu\varepsilon_{\mathrm{L}}\tilde{\xi}_{n+1}}\left\langle \tilde{L}_{\mathrm{An+1}}\right\rangle \tag{31}$$

553

554   where the $\tilde{F}$'s stand for the time discrete expressions of the loading surfaces in terms of

555   the basic variables; for instance $\tilde{F}_{\mathrm{Msn+1}}$ reads

556
$$\tilde{F}_{\mathrm{Msn+1}}(\mathbf{E}_{n+i}, \tilde{\mathbf{E}}_{\mathrm{Trn+i}}, \tilde{T}_{n+1}) = 2\mu \left|DEV(\mathbf{E}_{n+1} - \tilde{\mathbf{E}}_{\mathrm{Trn+1}})\right| - \sqrt{\frac{2}{3}}C_{\mathrm{M}}(\tilde{T}_{n+1} - M_{\mathrm{s}}),$$

557   while the $\tilde{L}$'s stand for the isothermal loading rates, e.g.,

558
$$\tilde{L}_{\mathrm{Mn+1}} = \frac{\partial \tilde{F}_{\mathrm{Mn+1}}}{\partial \mathbf{E}_{n+1}} : \mathbf{E}_{n+1}.$$

559   Note that within the context of the present strain-temperature space formulation the stress

560   tensor $\tilde{\mathbf{S}}_{n+1}$, does not appear in Eqs. (30) and (31), so that the (isothermal) problem is

29

561 reduced to solving these equations for the unknowns $\begin{bmatrix} \tilde{\mathbf{E}}_{\mathbf{Tr}n+1} \\ \tilde{\xi}_{n+1} \end{bmatrix}$. This problem can be solved

562 by means of a *three-step* predictor-corrector algorithm. The computational details

563 underlying the solution of the isothermal problem can be found in our previous work in

564 Panoskaltsis et al. [36] (see Section 4.1).

565 This provides the *initial update* of the internal variables, i.e.

$$566 \qquad \Gamma_n = \begin{bmatrix} \mathbf{E}_{\mathbf{Tr}n} \\ \tilde{\xi}_{1n} \end{bmatrix} \rightarrow \tilde{\Gamma}_{n+1} = \begin{bmatrix} \tilde{\mathbf{E}}_{\mathbf{Tr}n+1} \\ \tilde{\xi}_{n+1} \end{bmatrix}, \text{ for } \tilde{T}_{n+1} = T_n .$$

567

568 *Step 2: Non-isothermal inelastic problem at fixed configuration*

569 At this step, the total configuration, mediated herein by $\mathbf{F}_{n+1}$ - or equivalently by $\mathbf{E}_{n+1}$ -

570 remains fixed, while the solution of the isothermal problem is considered as an initial

571 condition, that is the known data at the beginning of this step are the elements of the set

$$572 \qquad \{\mathbf{E}_{n+1}, \tilde{T}_{n+1}, \mathbf{E}_{\mathbf{Tr}n}, \xi_n\},$$

573 while the application of the backward Euler scheme yields the following algorithm

$$574 \qquad 2\mu(\mathbf{E}_{\mathbf{Tr}\,n+1} - \mathbf{E}_{\mathbf{Tr}\,n}) = \sqrt{\frac{3}{2}}\varepsilon_{\mathbf{L}}\,(\xi_{n+1} - \xi_n)\left(\frac{\partial F_{n+1}}{\partial \mathbf{E}}\right)_{n+1} \tag{32}$$

$$575 \qquad \begin{aligned} \xi_{n+1} - \xi_n &= -\frac{\langle -F_{\mathbf{M}fn+1}F_{\mathbf{M}sn+1}\rangle}{|F_{\mathbf{M}fn+1}F_{\mathbf{M}sn+1}|}\frac{1-\xi_{n+1}}{F_{\mathbf{M}n+1}-2\mu\varepsilon_{\mathbf{L}}(1-\xi_{n+1})}\langle L_{\mathbf{M}n+1}\rangle \\ &\quad -\frac{\langle -F_{\mathbf{A}fn+1}F_{\mathbf{A}sn+1}\rangle}{|F_{\mathbf{A}fn+1}F_{\mathbf{A}sn+1}|}\frac{\xi_{n+1}}{F_{\mathbf{A}fn+1}+2\mu\varepsilon_{\mathbf{L}}\xi_{n+1}}\langle L_{\mathbf{A}n+1}\rangle \end{aligned} \tag{33}$$

$$576 \qquad c(T_{n+1} - \tilde{T}_{n+1}) = \dot{Q}_{en+1} + \dot{Q}_{\mathbf{Tr}n+1} - \frac{1}{\rho_{\mathrm{ref}}}DIV\mathbf{H}_{n+1} , \tag{34}$$

577 where

578
$$\dot{Q}_{en+1} = T_{n+1}[\frac{\partial^2 \Psi}{\partial T \partial E}\Big|_{n+1} : [(E_{n+1} - E_n) - (E_{Tm+1} - E_{Tm})],$$

579
$$\dot{Q}_{Trm+1} = -(\frac{\partial \Psi}{\partial E_{Tr}}\Big|_{n+1} : (E_{Trn+1} - E_{Trn}) + \frac{\partial \Psi}{\partial \xi}\Big|_{n+1} (\xi_{n+1} - \xi_n) + T_{n+1} \frac{\partial^2 \Psi}{\partial T \partial \xi}\Big|_{n+1} (\xi_{n+1} - \xi_n),$$

580 the F's stand for the time discrete expressions of the loading surfaces at time strep t_{n+1}

581 and the L's stand now for the *non-isothermal loading* rates, e.g.

582
$$L_{Mn+1} = \frac{\partial F_{Mn+1}}{\partial E_{n+1}} : (E_{n+1} - E_n) + \frac{\partial F_{Mn+1}}{\partial T_{n+1}} (T_{n+1} - \tilde{T}_{n+1}).$$

583 The solution of this algorithmic problem yields the values of the basic variables $\begin{bmatrix} E_{Trn+1} \\ T_{n+1} \\ \xi_{n+1} \end{bmatrix}$,

584 so that the second Piola-Kirchhoff stress tensor S can be determined by means of the

585 thermomechanical state equation

586
$$S_{n+1} = \lambda tr(E_{n+1} - E_{Tr\ n+1})1 + 2\mu(E_{n+1} - E_{Trn+1}), \tag{35}$$

587 Note that Eqs. (31) and (33) can be reduced further, depending on whether the (M) or

588 the (A) transformation is active (see [33, 36] for further details).

589

590 **REMARK 6** The proposed isothermal split has the disadvantage of not being

591 unconditionally stable. An alternative numerical treatment relies on the *isentropic split* -

592 see Armero and Simo [4]; see also Agelet de Saracibar et al. [1] - where unlike the present

593 case, the coupled problem is divided into *an isentropic mechanical phase in which the total*

594 *entropy is held constant*, followed by a *thermal phase at a fixed configuration*, which leads

595 to an unconditionally stable algorithm. In the present case and since we deal with

596 homogeneous problems, where the coupling between the governing equations is relatively

597 small, the stability problem is not an issue; as a result, the isothermal split seems to be

598 adequate.

599

600 *4.2 Numerical simulations*

601 *4.2.1 Simple shear*

602 The first problem we study is a standard one within the context of finite inelasticity and

603 is that of simple shear which is defined as

604
$$x_1 = X_1 + \gamma X_2, \quad x_2 = X_2, \quad x_3 = X_3,$$

605 where γ is the shearing parameter. In order to show the computational versatility enjoyed

606 by the model we work with three set of parameters. The first set is that reported in Boyd

607 and Lagoudas [7] for a generic SMA, that is

608
$$E_M = 13,000 \text{ MPa}, \ E_A = 30,000 \text{ MPa}, \ \nu = 0.3,$$
$$M_f = 5^o\text{C}, \ M_s = 23^o\text{C}, \ A_s = 29^o\text{C}, \ A_f = 51^o\text{C},$$
$$C_M = 11.3 \text{ MPa/}^o\text{C}, \ C_A = 4.5 \text{ MPa/}^o\text{C}, \ \varepsilon_L = 0.0635.$$

609 The second set of parameters is that reported in Auricchio et al. [5], for a commercial NiTi,

610 i.e.,

611
$$E_M = 24,600 \text{ MPa}, \ E_A = 31,000 \text{ MPa}, \ \nu = 0.33,$$
$$M_f = 250^o\text{K}, \ M_s = 265^o\text{K}, \ A_s = 276^o\text{K}, \ A_f = 291^o\text{K},$$
$$C_M = 10.50 \text{ MPa/}^o\text{K}, \ C_A = 5.5 \text{ MPa/}^o\text{K}, \ \varepsilon_L = 0.041.$$

612 while the third set of parameters is that given in Speicher et al. [49] for a $Ni_{50.8}Ti_{49.2}$ SMA,

613 that is

614
$$E_M = 38,200 \text{ MPa}, \ E_A = 48,500 \text{ MPa}, \ \nu = 0.42,$$
$$M_f = 218.5^o\text{K}, \ M_s = 258.15^o\text{K}, \ A_s = 258.15^o\text{K}, \ A_f = 288.15^o\text{K},$$
$$\varepsilon_L = 0.0475,$$

615 For this SMA, the remaining parameters C_M and C_A are considered to be equal to those

616 of the alloy discussed by Boyd and Lagoudas in [7].

617 The parameters of the non-isothermal part of the model are set equal *for all* SMAs to those

618 used in Müller and Bruhns [29], that is:

619 $\rho_{ref} = 6.45 \times 10^{-3}$ k/m mm^2, $\alpha_t = 8.8 \times 10^{-6} 1/^\circ$ K, c $= 837.36$ J/kg$^\circ$K
$\Delta u^* = u_0^{*A} - u_0^{*M} = 16800.0$ J/kg, $\Delta s^* = s_0^{*A} - s_0^{*M} = 64.50$ J/kg$^\circ$K,
$\bar{u}_0 = 4264.5$ J/kg, $\bar{s}_0 = 11.5$ J/kg$^\circ$K.

620 Within this simulation we examine the ability of the model in predicting pseudoelastic

621 phenomena under non-isothermal conditions. For this purpose, an adiabatic testis

622 considered. We further assume that due to the dynamic rates resulting in adiabatic response,

623 heat exchanges due to conduction, convection and radiation can be neglected in comparison

624 to the material heating/cooling induced by the inelastic (transformation) contribution to the

625 heating $(\dot{Q}_{Tr})$, a fact which leads to thermomechanical processes that can be considered as

626 homogeneous (see Rosakis et al. [47]). Accordingly, within this simulation the temperature

627 evolution equation reads

628 $$c\dot{T} = -(\frac{\partial \Psi}{\partial \mathbf{E_{Tr}}} : \dot{\mathbf{E}}_{Tr} + \frac{\partial \Psi}{\partial \xi}\dot{\xi}) + T\frac{\partial^2 \Psi}{\partial T \partial \xi}\dot{\xi}.$$

629 Our purpose in this example is to discuss a complete stress-induced transformation cycle

630 at a temperature $T_0 = 60^\circ C > A_f$, where the SMA material exhibits pseudoelastic response.

631 The stress-deformation curves for this finite shear problem are shown in Figs. 1, 2 and 3

632 while the corresponding temperature-deformation curves are depicted in Fig. 4. Consistent

633 with the adiabatic response of an SMA material at temperature $T_0 > A_f$ (see, e.g., Grabe

634 and Bruhns [13]), the model predicts heat generation during the forward (*M*) transformation

33

635 and heat absorption during the reverse (A) transformation. Moreover, we note that at the

636 end of the forward (M) the model predicts that the temperature increase is the same for the

637 three alloys in question. This response is consistent with the experimentally observed one

638 (see, e.g., Peyroux et al. in [39]), and relies on the fact that, unlike the case of metals, in

639 SMAs the dissipated mechanical work $-(\frac{\partial \Psi}{\partial \mathbf{E_{Tr}}} : \dot{\mathbf{E}}_{Tr} + \frac{\partial \Psi}{\partial \xi} \dot{\xi})$, remains very small

640 compared to the latent heat $T \frac{\partial^2 \Psi}{\partial T \partial \xi} \dot{\xi}$ due to phase changes; note that within the context of

641 present problem the latent heat is dominated by the non-isothermal part of the model which

642 has been considered the same for the three alloys.

643 A comparison between the corresponding isothermal and adiabatic responses for the

644 alloy discussed by Auricchio et al. in [5] is illustrated in Figs. 5 and 6. By referring to these

645 results we note that, under adiabatic conditions the forward (M) transformation occurs at

646 higher levels of stress, than the isothermal one. This fact has its origins to the temperature

647 increase which tries to stabilize the austenite and inhibit the transformation. As a result, a

648 higher level of stress is required to induce the forward (M) transformation. Moreover, by

649 referring to Fig. 6 we note that in general temperature changes retard both the forward (M)

650 and the reverse (A) transformations. In the latter case, this result has to be attributed to the

651 temperature decrease during the reverse transformation which now tries to stabilize the

652 martensite phase.

653

654 *4.2.2 Uniaxial tension: validation of the model against actual experimental data*

655   In order to verify further the ability of the proposed framework for simulating isothermal

656   (quasi-static) and adiabatic (dynamic) responses we consider a uniaxial tension problem.

657   This problem is defined as

658    $$x_1 = (1+\lambda)X_1, \; x_2 = (1+\omega)X_2, \; x_3 = X_3 \, ,$$

659   where $1+\lambda$ and $1+\omega$ are the straining parameters (principal stretches) along the axial and

660   transverse directions, respectively. Note that in the infinitesimal case, λ and ω are equal to

661   the corresponding principal normal strains ε_{11} and ε_{22}. Our purpose here is to compare the

662   predictions of the proposed model with the experimental results reported by Auricchio et

663   al. in [5]; see also Fig. 3 in [26]. The basic (isothermal) parameters are those used in the

664   simple shear problem, while the remaining parameters underlying the dynamic response

665   are set equal to

666    $\varepsilon_{\mathrm{L}} = 0.038, \; \Delta u^* = 5800.0$ J/kg, $\Delta s^* = 64.50$ J/kgK,
       $\bar{u}_0 = 265$ J/kg, $\bar{s}_0 = 10.0$ J/kgK.

667   As in the simple shear problem the material is subjected to a stress (loading-unloading)

668   cycle a temperature $T_0 = 295 \; {}^{\circ}\mathrm{K}(> A_f)$. The results are shown in Fig. 7. By referring to

669   these results, we observe that the proposed model can capture adequately both the change

670   in slope and the change of the hysteresis loop both in the case of quasi-static ($\tau = 1000$ sec,

671   where $\tau =$ is time of a loading-unloading cycle) and dynamic loading ($\tau = 1$ sec - see also

672   Fig. 3 in [26]). We also observe that the simple linear expression for the evolution of the

673   material martensite fraction ξ used herein cannot capture precisely the shape of the

674   transformation branches. Nevertheless, this does not consist a serious drawback, since this

675   expression - recall section 2.1 - can be replaced adequately by a more sophisticated (e.g.

676   polynomial, exponential, hyperbolic) one; further details on the selection of the evolution

677   function for a two-shape memory alloy can be found in [39].

678   As a further illustration, in Figs 8 and 9, we show the effect of the (basic) thermal

679   parameters of the model in the stress-deformation curve. It is observed that, while the effect

680   of $\bar{u}_0$ is practically negligible, the thermal parameter Δu^* plays an eminent role in the

681   predicted behavior upon controlling the slope of the stress-deformation curve.

682

683   *4.2.3 Shape memory effect*

684   As a next simulation we will evaluate the ability of the model in predicting the shape

685   memory effect. For this purpose, we revisit the uniaxial tension test. For this problem the

686   basic material parameters are set equal to those given in [5], while the material stiffness is

687   assumed to be constant ($E = E_A = 30,000 \text{Mpa}$).

688   The isothermal stress-strain curves for three different material temperatures

689   ($T_0 = 55^o\text{C} = A_f$, $A_f > T_0 = 40^o\text{C} > A_s$, $A_s > T_0 = 28^o\text{C}$) are shown in Fig. 10. By referring

690   to this figure for $T_0 = A_f$, the ability of the model in predicting pseudoelastic phenomena

691   under isothermal conditions is verified; note that since the temperature has been set exactly

692   equal to A_f, the reverse transformation ends at zero stress. The isothermal tests for

693     $A_f > T_0 > A_s$ and $A_s > T_0$ are conducted in order to show the ability of the model in

694   predicting the shape memory effect. In the first of them, upon loading the (*M*)

695   transformation is activated. Upon unloading and since the temperature is less than the

696   temperature required for the complete reverse transformation at zero stress, the two phases

697   coexist and permanent deformations appear. However, as it will be clear in the subsequent,

698   these deformations can be recovered after increasing the temperature. In the last test, since

699   the temperature has been set at a value less than the austenite start temperature at zero

700   stress, at the end of the stress cycle the material is completely in the martensite phase. This

701   results in the appearance of large permanent deformations, which are manifested by the

702   maximum inelastic strain ε_L. Nevertheless, like the previous test this deformation may be

703   eliminated upon heating.

704   For the material heating problem, we assume thermal boundary conditions corresponding

705   to *convective heat exchange between the specimen and the surrounding medium* on the free

706   faces (with area *A*) of the specimen; each face is assumed to have a unit area. In this case

707   the normal heat flux $\mathbf{H_u}$, is given by Newton's' law of cooling (see, e.g., [48]) as

708   $$\mathbf{H_u} = hA(\mathrm{T}_\infty - \mathrm{T}_0),$$

709   where   *h*   stands   for   the   convection   coefficient   which   is   chosen   to   be

710   $h = 20 \cdot 10^{-3}$ N/mm°K , and T_∞ is the surrounding medium temperature. By assuming

711   that the size of the material tested is small, the contribution to the material heating due to

712   the heat conduction can be neglected; a similar assumption has been also made by

713   Auricchio et al. [5]. As a result, in the absence of phase transformations the material

714   behaves as a *rigid body hear convector*; the corresponding temperature evolution

715   equation reads

716   $$c\dot{\mathrm{T}} = \dot{Q}_{\mathbf{Tr}} - \frac{1}{\rho_{\mathrm{ref}}}\mathbf{H_u}.$$

717   The results of this test are illustrated in Fig. 11 where the strain along $X_1 -$ axis is plotted

718   versus the surrounding medium temperature.

719

720   *4.2.4 Thermally induced martensitic transformations at zero stress*

721   As a further simulation we show the ability of the model in predicting pseudoelastic

722   response under a thermal cycle. As in the simple shear problem, all numerical tests are

723   performed with the specimen being initially in the austenite phase, while the temperature

724   is set equal to 333.0°C, that is $T_0 > A_r$. Our purpose here is to discuss a complete

725   thermally-induced transformation cycle at zero stress. The results, for this cycle are

726   shown in Figs. 12 and 13. On cooling, initially the material remains in the austenite phase.

727   As cooling is continuing and the temperature attains M_s, that is the material point reaches

728   the initial loading surface for the forward transformation at zero stress $(F_{Ms} = 0)$, the

729   phase transformation starts and is continued by a sudden burst of strain at the maximum

730   inelastic one (ε_L). Nevertheless, as in the previous case, this strain can be recovered upon

731   heating the material back to its initial temperature.

732

733   *4.2.5 Thermomechanical response under a strain cycle*

734   Another interesting example arises in the case where a SMA material is subjected to a

735   *strain cycle.* For this purpose, we revisit a problem discussed within an isothermal setting

736   in Panoskaltsis et al. [36]; (see also [39]). This problem is suggested in Meyers et al. [25]

737   and deals with a square element of size $H \times H$, which is imposed into a strain cycle by

738   *rotating both upper corners along a cycle of radius r* (see Fig. 1 in [25]). Accordingly, the

739   element even though is submitted to both an extension along the X_2 axis, and $1-2$ shear,

740   it preserves its original (parallelogram) shape. This problem is defined as follows:

$$x_1 = X_1 + \frac{\sin\varphi \, {}^r\!/_H}{1 + (1 - \cos\varphi)\, {}^r\!/_H} X_2,$$

741

$$x_2 = 1 + (1 - \cos\varphi)\, {}^r\!/_H \, X_2,$$

$$x_3 = X_3.$$

742   For this problem the material parameters are set equal to those given in Auricchio et al.

743   [3], while as in the shape memory effect problem, the material stiffness is assumed to be

744   constant and equal to the austenite stiffness. The corresponding stress-angle of rotation

745   curves for ${}^r\!/_H = 0.02$ are plotted in Fig. 14, while the temperature evolution is plotted in

746   Fig. 15. By referring to these figures, we realize that at the end of the strain cycle, the

747   stresses go back to zero and the material, by obtaining its original stress-free state, is giving

748   the false impression that is elastic. However, this recovery has its origins in the martensitic

749   transformations, since as it is clear from Fig. 16, where the variation of material martensite

750   fraction is plotted versus φ, both (*M*) and (*A*) transformations have been (partially)

751   activated during this strain cycle. This response is dubbed in Panoskaltsis et al. [36] as *non-*

752   *conventional pseudoelastic*, in the sense that, unlike the previous (conventional)

753   simulations where the material was subjected to stress cycles, the material is now subjected

754   to a strain cycle; however, the exhibited response is identical.

755   Comparing this response to the isothermal one, which is also depicted in Fig. 16, we note

756   the *inhibition of the forward transformation due to the temperature increase.* In this case -

757   compare with Figs. 5 and 6 - the total strain applied, even though is adequate to induce the

758   full isothermal phase transformation, due to material heating becomes inadequate to

759   introduce the non-isothermal one before unloading begins. This pattern of non-

760   conventional response is better illustrated in Fig. 17, where the isothermal, as well as the

761   non-isothermal cases, are considered for three different values of the ratio r/H.

762

763   4.2.6 *Inhibition of the forward transformation at high temperatures*

764   As an additional pattern of non-conventional response, we consider a case where the

765   forward (*M*) transformation is inhibited due to the material heating (see, e.g., Olson and

766   Cohen [31]; McKelvey and Ritchie [24]). This case may appear when the material is

767   stressed at a relatively high temperature T_0, which is near the limit M_d for the existence

768   of stress induced martensite. In order to make this matter more precise, we revisit the

769   simple shear problem and we consider the case where the material discussed in [5] is

770   stressed at *three relatively high temperatures*, that is $T_0 = 70^oC$, $T_0 = 90^oC$ and

771      $T_0 = 110^oC$. The results are illustrated in Figs. 18, 19 and 20. By comparing these results

772   with those of Fig. 5 and 6 and since the austenite is more stable at high temperatures, we

773   verify that a higher level of stress is required to induce the forward transformation; more

774   importantly, we note that the temperature increase during the transformation may inhibit

775   the phase transformation if the critical temperature M_d is reached. More specifically, we

776   observe that unlike the first case $(T_0 = 70^oC)$, where the material temperature remains

777   always below M_d and the full forward transformation is activated, in the remaining cases

778     $(T_0 = 90^oC; T_0 = 110^oC)$, the material temperature in the course of the transformation

779   exceeds M_d and *the austenite suddenly becomes stable*, so that the *transformation stops*.

780   If this is the case, the two phases coexist $(0 < \xi < 1)$ and the material upon further stressing

781   behaves elastically.

782

783

784   *4.3 Thermomechanical response of an SMA wire under uniaxial extension*

785

786   As a final simulation we discuss the thermomechanical response of a SMA wire under

787   uniaxial extension, which in general constitutes a very active area of research within the

788   SMAs literature (see, e.g., Zakiet al. [56]; Mirzaeifar et al. [26]; Andani et al. [3]; see also

789   Leo et al. [19]). More specifically we place special emphasis in the *heat equation (diffusion*

790   *equation)* initial boundary value problem (IBVP), which underlies the temperature

791   evolution in an SMA wire in the course of phase transformations. The same problem has

792   been also discussed within the context of classical non-isothermal metal plasticity by

793   Kamlah and Haupt [16].

794   Accordingly, we assume an SMA wire of length L, which is subjected in uniaxial tension;

795   we restrict our attention to *small temperature deviations* $T = \mathrm{T} - \mathrm{T}_0$ from the reference

796   temperature. We assume also that the lateral surface of the wire is adiabatically isolated so

797   that heats flow along $X_1 -$ direction only. Then by denoting by k the thermal conductivity

798   coefficient and by $u(t)$ the *heat source (sink density)*, the temperature evolution equation

799   can be written in the (standard) heat equation form, as

800
$$\frac{\partial T(X^1,t)}{\partial t} = m^2 \frac{\partial (X^1,t)}{\partial X_1^2} + u(t),$$

801   where $m^2 = \dfrac{k}{c\rho_{ref}}$, stands for the thermal diffusivity of the material. In order to formulate

802   the corresponding IBVP, at the beginning the temperature is set equal to T_0, while we

803   assume that the heat transfer from the testing machine to the wire is being done without

804   any resistance, which means that we can consider that the temperature in the surfaces of

805   the wire remains equal to T_0. In this case, the heat source term $u(t)$ is equal to $\rho_{ref}\dot{Q}_{\mathrm{Tr}}$. On

806   the basis of these assumptions, the *non-homogeneous heat equation* IBVP can be stated as

$$\frac{\partial T(X^1,t)}{\partial t} = m^2 \frac{\partial (X^1,t)}{\partial x_1^2} + \rho_{ref}\dot{Q}_{\mathrm{Tr}}(t),$$

807    $$\text{Boundary conditions: } T(0,t)=0, \ T(\mathrm{L},t)=0,$$
$$\text{Initial condition: } T(x_1,0)=0.$$

808   The solution of this problem can be pursued by a semi-analytical method (see also Kamlah

809   and Haupt in [16]) by noting that at the isothermal step (step 1) the equilibrium equation is

810   trivially satisfied and the stress field within the wire is homogeneous. Then, the heat

811   conduction problem (step 2) can be solved by a separation of variables method, which leads

812   to the following expression for the thermal field

$$T(X_1,t) = \sum_{n=1}^{\infty} T_n(t) X_n(X_1),$$

814   where

$$T_n(t) = e^{-\lambda_n m^2 t} \int_0^t a_n(\tau) e^{\lambda_n m^2 t} dt,$$

816   in which λ_n and X_n are the eigenvalues and the eigen-functions of the associated Sturm -

817   Liouville problem, obtained as

$$\lambda_n = \frac{n\pi^2}{L}, \ X_n = \sin\frac{n\pi X_1}{L},$$

819   and

820
$$a_n(\tau) = u(t) \frac{\int_0^L X_n(X_1)dx_1}{\int_0^L X_n^2(X_1)dx_1}.$$

821   The parameters used for this problem are those reported in [7], while the reference

822   temperature is set equal $T_0 = 60^\circ C > A_f$. The length L of the wire is assumed to be 10 cm

823   and the thermal conductivity coefficient k is set equal to $20\frac{W}{m^\circ K}$.

824   The basic results are shown in Figs. 21 and 22. In particular Fig. 21 depicts the time

825   evolution of the heat source term $u(t)$ as derived from the inelastic problem under frozen

826   thermal field, while Fig. 22 shows the time evolution of the temperature field along the

827   length of the wire, as derived by considering the heat source as an input for the heat

828   conduction problem. By referring to the results of Fig.22, we note that the temperature

829   distribution along the length of the wire has the shape of the half of a sinus function. Further

830   it is noted that the temperature-time curve has the same qualitative characteristics, with

831   those of the (local) simple shear problem. As a further illustration, in Figs. 23 and 24, we

832   show the effect of the (basic) thermal parameters Δu^* and $\bar{u}_0$ of the model, by plotting the

833   temperature evolution versus time at the mid-point $(X_1 = \frac{L}{2})$ of the wire. As expected –

834   recall the analysis provided in Section 4.2.2 - while the effect of $\bar{u}_0$ is negligible, this is not

835   the case for parameter Δu^*. The latter, affects the temperature evolution (see Fig. 23) and

836   eventually the stress developed during transformations (see also Fig. 8).

837

838   **5   Closure**

43

839

840 The basic impact of this paper lies on the development of a general inelastic framework

841 which accounts for the development of sound constitutive models describing the complex

842 response of shape memory alloys under general states of deformation and temperature

843 conditions. More specifically and from a theoretical standpoint in this paper:

844 *(i)* We have revisited the multi-surface formulation of generalized plasticity and

845 we have extended it to a covariant one, that is, we have presented it in a setting

846 where the basic equations have an identical form in both the reference and the

847 spatial configurations.

848 *(ii)* We have implemented - possibly for first time in the literature of shape memory

849 alloys - an invariance (symmetry) principle, namely that of the covariance of

850 the referential energy balance equation, for the derivation of the

851 thermomechanical state equations.

852 *(iii)* Furthermore, on studying the local balance of energy equation, we have derived

853 several expressions for the temperature changes which occur in the course of

854 phase transformations.

855 Therefore, the present formulation is more general and more powerful than the previous

856 ones developed in [33, 38].

857 Moreover, from a computational standpoint in this paper:

858 *(i)* On the basis of an isothermal split we have discussed a (local) time

859 integration scheme for the numerical implementation of a generalized

860 plasticity based model. The scheme is rather general and can account for

861 almost all thermomechanically coupled problems.

44

862   *(ii)*   We have demonstrated the ability of the framework in describing the

863   response of SMAs during phase transformations by a set of representative

864   These examples are ranging from a standard simple shear problem to full

865   scale three-dimensional simulations where the material exhibits non-

866   conventional pseudoelastic response. We have paid special attention to cases

867   where phase transformations may be retarded of even inhibited due to

868   material self-heating/cooling effects.

869   *(iii)*   We have also studied a non-local problem, namely the one of the

870   heating/cooling of an SMA wire under uniaxial tension.

871   Finally, it is emphasized, that since the present formulation considers the additive

872   decomposition of the finite strain tensor into elastic and inelastic (transformation induced)

873   parts, besides being conceptually simple, provides a framework within which plethora of

874   constitutive models developed within the context of infinitesimal theory and met

875   frequently within the SMA's literature - see, e.g., [40, 18, 33, 27] - can be extended to the

876   finite deformation regime in a straight forward manner.

877

878
879   **References**
880
881

882   [1] Agelet de Saracibar, C., Cervera, M., Chiumenti, M.: On the constitutive modeling
883   of coupled thermomechanical phase-change problems. Int. J. Plast. **17**, 1565-1622
884   (2001)
885   [2] Anand, L., Gurtin, M. E.: Thermal effects in the superelasticity of crystalline
886   shape- memory materials. J. Mech. Phys. Solids **51**, 1015-1058 (2003)
887   [3] Andani, T. A., Alipour, A., Elahinia, M.: Coupled rate-dependent superelastic
888   behavior of shape memory alloy bars induced by combined axial-torsional
889   loading: A semi-analytic modeling. *J. Intel. Mat. Sys. Struct.*,**24,** 1995-2007
890   (2013)

[4] Armero, F., Simo, J. C.: A-priori stability estimates and unconditionally stable product formula algorithms for non-linear coupled thermoplasticity. Int J. Plast. **9,** 149-182 (1993)

[5] Auricchio, F., Fugazza, D., DesRoches, R.: Rate-dependent thermo-mechanical modeling of superelastic shape-memory alloys for seismic applications. J. Intell. Mater. Systems Struct. **19**, 47-61 (2008)

[6] Ball, J. M., James, R. D.: Fine phase mixtures and minimizers of energy. Arch. Rat. Mech. Anal. **100**, 13-52 (1987)

[7] Boyd, J. G., Lagoudas, D. C.: A thermodynamic constitutive model for shape memory alloy materials. Part I. The monolithic shape memory alloy, Int. J. Plast. **12**, 805-842 (1994)

[8] Boyd, J. C., Lagoudas, D. C.: Thermodynamical response of shape memory composites. J. Intell. Mater. Systems Struct. **5**,333-346 (1994)

[9] Christ, D., Reese, S.: A finite element model for shape - memory alloys considering thermomechanical couplings at large strains. Int. J. Solids Struct. **46**, 3694-3709 (2009)

[10] Earman, J.: Laws, symmetry and symmetry breaking: Invariance, conservation principles and objectivity. Phil. Sci.*,* **71**, 1227-1241(2004)

[11] Fosdick, R.L., Serrin, J.: Global properties of continuum thermodynamic processes. Arch. Rat. Mech. Anal., **59**, 97-109 (1975)

[12] Ganghoffer, J. F.: Symmetries in mechanics: from field theories to master responses in the constitutive modeling of materials. [In]: *Similarity and Symmetry Methods, Applications in Elasticity and Mechanics of Materials*, J. F. Ganghoffer, I Mladenov [eds], Springer, 271-351 (2014)

[13] Grabe, C., Bruhns, O.T.: On the viscous and strain rate dependent behavior of polycrystalline NiTi. Int. J. of Solids and Struct. **45**, 1876-1895 (2008)

[14] Holzapfel, G. A.: Nonlinear solid mechanics. A continuum approach for engineering, John Wiley & Sons, West Sussex, England (2000)

[15] Huo, Y., Müller, I.: Nonequilibrium thermodynamics of pseudoelasticity. Continuum Mech. Thermodyn. **5**, 163-204 (1993)

[16] Kamlah, M., Haupt, P.: On the macroscopic description of stored energy and self heating during plastic deformation. Int. J. Plast. **13**, 893 - 911 (1998).

[17] Lagoudas, D. C., Bo, Z., Qidwai, M. A.: A unified constitutive model for SMA and finite element analysis of active metal matrix composites. Mech. Comp. Matls Struct. **3**, 153-179 (1996)

[18] Leclercq, S., Lexcellent, C.: A general macroscopic description of the thermomechanical behavior of shape memory alloys. J. Mech. Phys. Solids, **44**, 953- 980 (1996)

[19] Leo, P. H., Shield, T. W., Bruno, O. P.: Transient heat transfer effects on the pseudoelastic behavior of shape-memory wires. Acta Metall. Mater. **41**, 2477-2485 (1993)

[20] Lu, Z. K., Weng G. J.: Martensitic transformation and stress-strain relations of shape-memory alloys.J. Mech. Phys. Solids **45**, 1905-1921 (1997)

[21] Lubliner, J.: Non-isothermal generalized plasticity. In: Thermomechanical Couplings in solids, eds. H. D. Bui and Q. S. Nyugen, 121-133 (1987)

936 [22] Lubliner, J., Auricchio, F.: Generalized plasticity and shape memory alloys. Int. J. Solids Struc. **33**, 991-1004 (1996)

938 [23] Marsden, J. E., Hughes, T. J. R.: Mathematical foundations of elasticity, Dover Publications, New York (1994)

940 [24] McKelvey A. L., Ritchie, R. O.: On the temperature dependence of the superelastic strength and the prediction of the theoretical uniaxial transformation strain in Nititol. Phil. Mag. **80**, 1759-1768 (2000)

943 [25] Meyers A, Xiao H, Bruhns O.: Elastic stress ratcheting and corotational stress rates. Technisce Mechanic **23**, 92-102 (2003)

945 [26] Mirzaeifar, R., DesRoches, R., Yavari, A.: Analysis of the rate-dependent coupled thermomechanical response of shape memory alloy bars and wires in tension. Continuum Mech. Thermodyn. **23**, 363-385 (2011)

948 [27] Morin, C., Moumni, Z., Zaki, W.: Thermomechanical coupling in shape memory alloys under cyclic loadings: Experimental analysis and constitutive modeling. Int. J. Plast. **27**, 1959-1980 (2011)

951 [28] Müller, I.: On the size of the hysteresis in pseudoelasticity. Continuum Mech. Thermodyn. **1**, 125-142 (1989)

953 [29] Müller, C., Bruhns O.T.: A thermodynamic finite-strain model for pseudoelastic shape memory alloys. Int. J. Plasticity **22**, 1658-1682 (2006)

955 [30] Naghdi, P. M.: A critical review of the state of finite plasticity. Z. Angew. Math. Phys. **41**, 315-387 (1990)

957 [31] Olson, G. B., Cohen, M.: Kinetics of strain-induced martensitic nucleation. Metal. Trans. A **6A**, 791-795 (1975).

959 [32] Panoskaltsis, V. P.: Mechanics of shape memory alloys - Constitutive modeling and numerical implications. In: Shape Memory Alloys - Processing, Characterization and Applications, Dr. Fransisco Manuel Braz Fernandes (ed) ISBN: 978-953-51-1084- 2, In Tech DOI 10.5772/52228 (2013)

963 [33] Panoskaltsis, V. P., Bahuguna, S., Soldatos, D.: On the thermomechanical modeling of shape memory alloys. Int. J. Non-Linear Mech. **39**, 709-722 (2004)

965 [34] Panoskaltsis, V. P., Soldatos, D., Triantafyllou, S., P.: Generalized plasticity theory for phase transformations, 11th International conference on the mechanical behavior of materials, M. Guagliano ed. Milano, Italy, 5-9 June 2011, Procedia engineering, 3104-3108 (2011)

969 [35] Panoskaltsis, V.P., Soldatos, D., Triantafyllou, S.P. A new model for shape memory alloy materials under general states of deformation and temperature conditions. 7th GRACM International Congress on Computational Mechanics, A.G. Boudouvis and G.E. Stavroulakis eds., 30 June- 2 July 2011, Athens, Greece.

973 [36] Panoskaltsis, V.P., Polymenakos, L.C., Soldatos, D. The concept of physical metric in the thermomechanical modeling of phase transformations with emphasis on shape memory alloy materials. ASME J. Eng. Mater. Technol., 135, 2, 021016 (Apr. 02, 2013) doi: 10.1115/1.4023780, 2013.

977 [37] Panoskaltsis, V. P., Soldatos, D.: A phenomenological constitutive model of non-conventional elastic response", Int. J. App. Mech., **5**, 1350035(2013)

979 [38] Panoskaltsis, V. P., Soldatos, D., Triantafyllou, S., P.: On phase transformations in shape memory alloy materials and large deformation generalized plasticity. Continuum Mech. Thermodyn. **26**, 811-831 (2014)

[39] Panoskaltsis, V. P., Polymenakos, L. C., Soldatos,: Large deformation constitutive theory for a two-phase shape memory alloy. *Engng. Trans.*, **62**, 355-380 (2014)

[40] Peyroux, R., Chrysochoos, A., Light, C., Löbel, M.: Thermomechanical couplings and pseudoelasticity of shape memory alloys. Int. J. Engrg. Sci. **36**, 489-509 (1998)

[41] Rahuadj, R., Ganghoffer, J. F. and Cunat, C.: A thermodynamic approach with internal variables using Lagrange formalism. Part I: General framework. Mech. Res. Comm. **30**, 109–117 (2003)

[42] 40. Rahuadj, R., Ganghoffer, J. F. and Cunat, C.: A thermodynamic approach with internal variables using Lagrange formalism. Part 2: Continuous symmetries in the case of the time-temperature equivalenceMech. Res. Comm.**30**, 119–123 (2003)

[43] Raniecki, B., Lexcellent, C. Tanaka, K.: Thermodynamic models of pseudoelastic behaviour of shape memory alloys. Arch. Mech. **44**, 3, 261-284 (1992)

[44] Raniecki, B., Lexcellent, C.: RL models of pseudoelasticity and their specification for some shape memory solids. Eur. J. Mech. A/Solids **12**, 1, 21-50 (1994)

[45] Raniecki, B., Lexcellent, C.: Thermodynamics of isotropic pseudoelasticity in shape memory alloys. Eur. J. Mech. A/ Solids **17**, 185-205 (1998)

[46] Romero, I.: A characterization of conserved quantities in non-equilibrium thermodynamics. Entropy **15**, 5580-5596 (2013).

[47] Rosakis, P., Rosakis, A. J., Ravichandran, G., Hodowany, J.: A thermodynamic internal variable model for partition of plastic work into heat and stored energy in metals. J. Mech. Phys. Solids **48**, 581-607 (2000)

[48] Simo, J. C., Miehe, C.: Associative couple thermoplasticity at finite strains: Formulation, numerical analysis and implementation. Comput. Methods Appl. Mech.Eng.**98**, 41-104 (1992)

[49] Speicher, M., Hodgson, D. E., DesRoches, R., Leon, R. T.: Shape memory alloy tension/compression device for seismic retrofit of buildings. J. Matls Eng. Performance 18, 746-753 (2009)

[50] Smallman, R. E., Bishop, R. J.: Modern physical metallurgy and materials engineering, 6th Edition, Butterworth - Heinemann, Stoneham, MA (2000)

[51] Stumpf, H., Hoppe, U.: The application of tensor analysis on manifolds to nonlinear continuum mechanics - Invited survey article. Z. Agrew. Math. Mech. **77**, 327-339 (1997)

[52] Thamburaja, P.: A finite-deformation-based theory for shape-memory alloys Int. J. Plasticity **26**, 1195-1219 (2010)

[53] Yavari, A., Marsden, J.E., Ortiz, M.: On spatial and material covariant balance laws in elasticity. J. Math. Phys. **47**, 1-53 (2006).

[54] Yin, Y. M., Weng, G. J.: Micromechanical study of thermomechanical characteristics of polycrystals shape-memory alloy films. Thin solid films, **376**, 198-207 (2000)

[55] Yu, C., Kang, G., Kan, Q., Zhu, Y.: Rate dependent cyclic deformation of super-elastic NiTi shape memory alloy: Thermo-mechanical coupled and physical mechanism- based constitutive model. *Int. J. Plast.,***72**, 60-90 (2015)

[56] Zaki, W., Morin, C., Moumni, Z.: A simple 1D model with thermomechanical coupling for superelastic SMAs. In: IOP Conf. Series: Materials Science and Engineering 10, 021149 (2010)

[57] Ziołkowski , A. Three-dimensional phenomenological thermodynamical model of pseudoelasticity of shape memory alloys at finite strains. Continuum. Mech. Thermodyn. **19**, 379-398 (2007)

LIST OF FIGURES
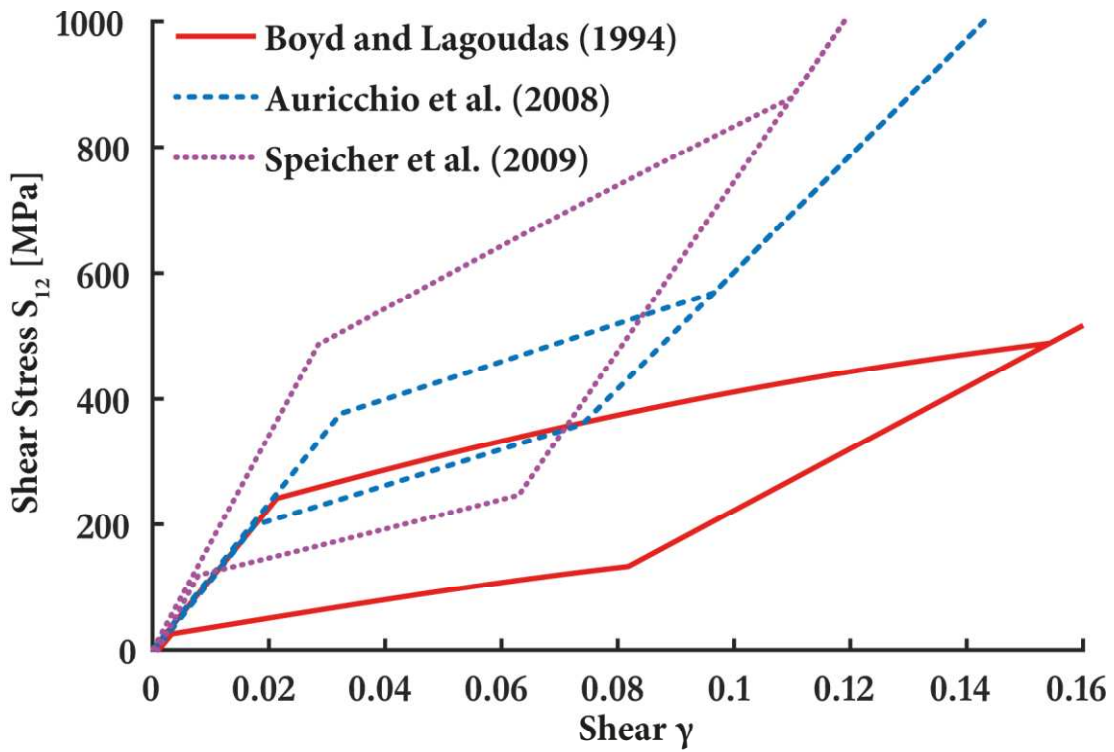
Figure 1: Finite Shear: Shear stress S_{12} vs. shear strain γ.
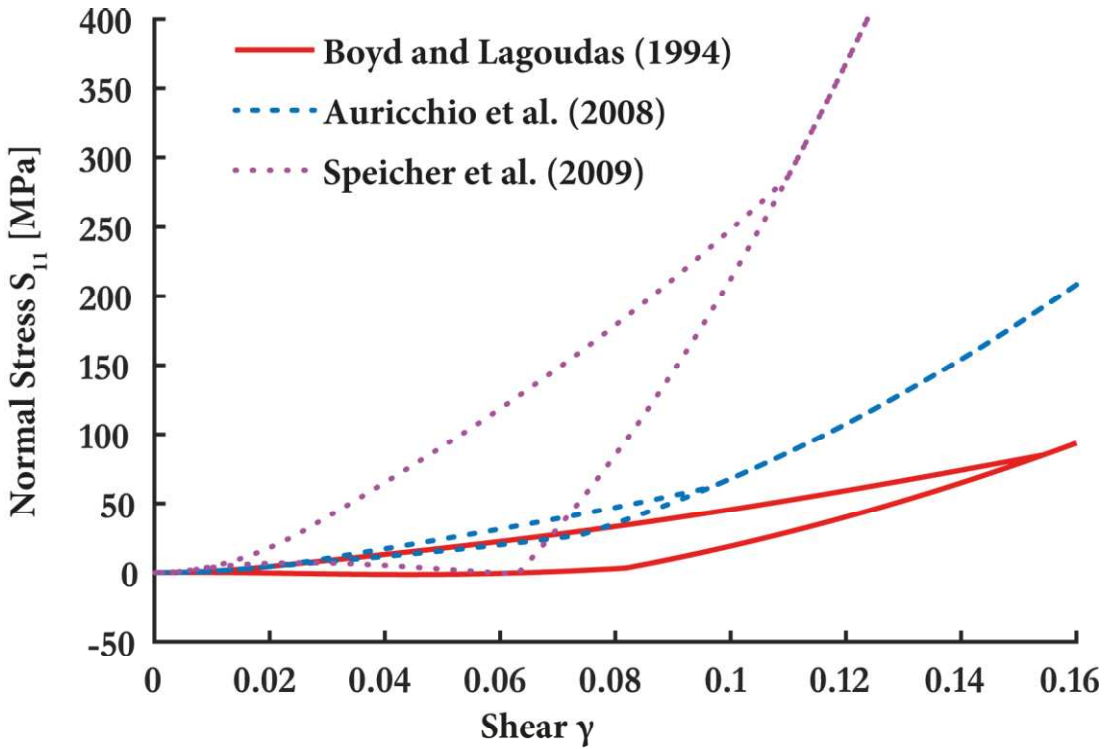
1047
1048 Figure 2: Finite Shear: Normal stress S_{11} vs. shear strain γ.
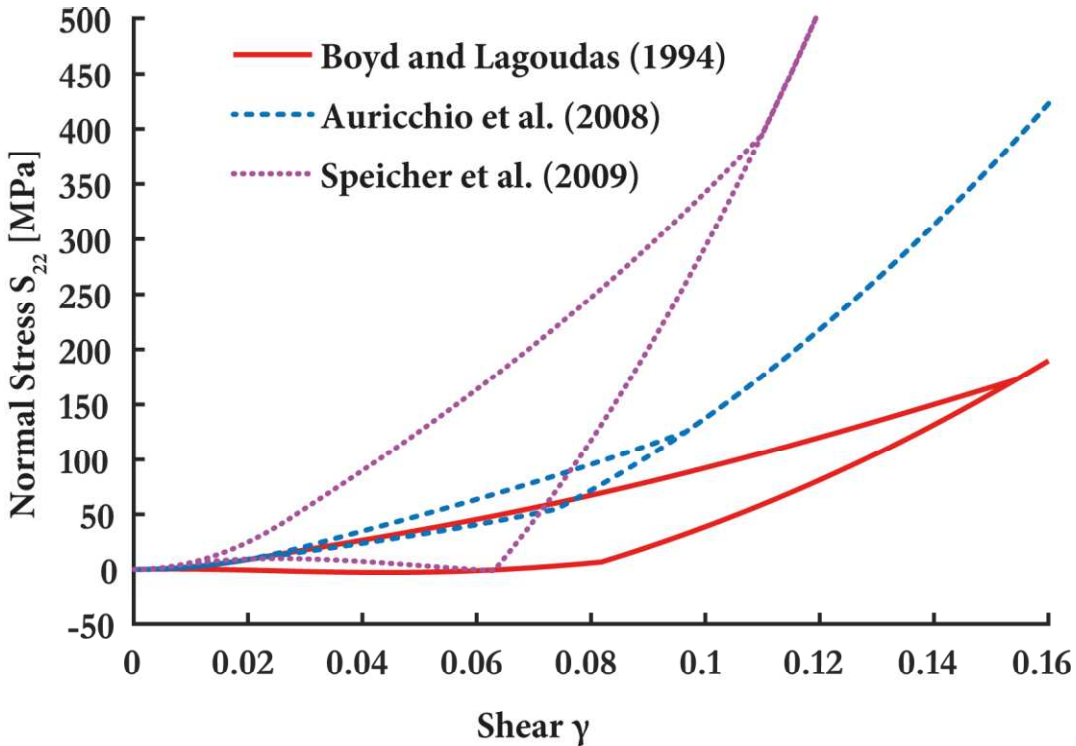
1049
1050 Figure 3: Finite Shear: Normal stress S_{22} vs. shear strain γ.

50
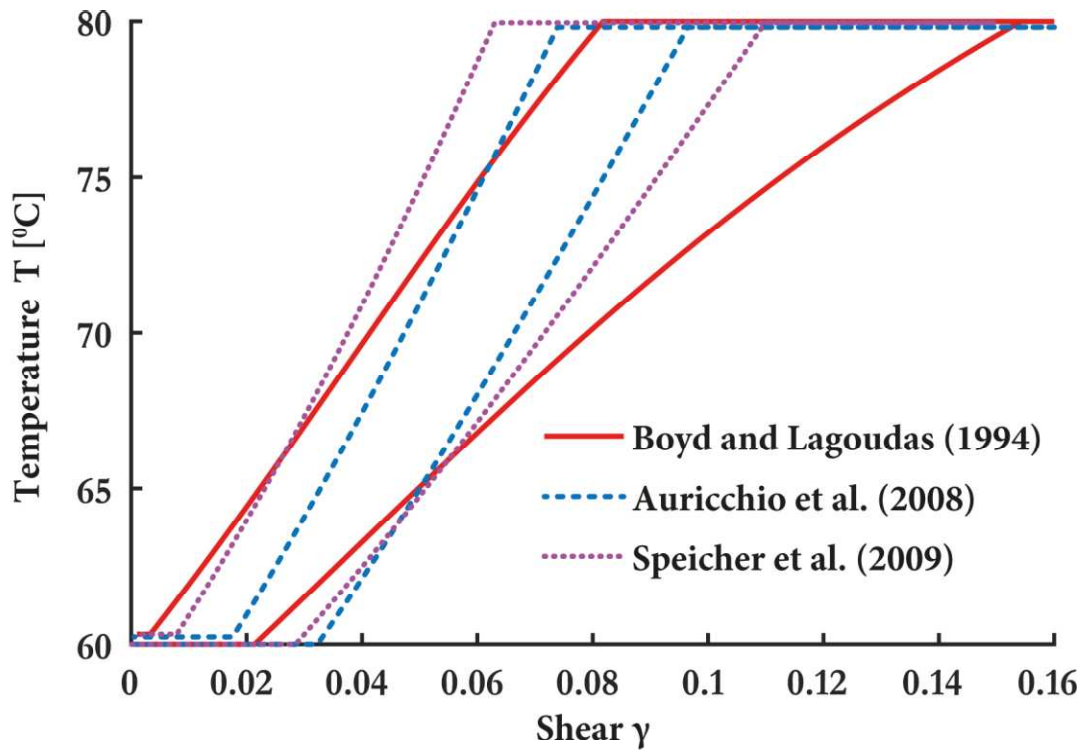
Figure 4: Finite Shear: Temperature T vs. shear strain γ.
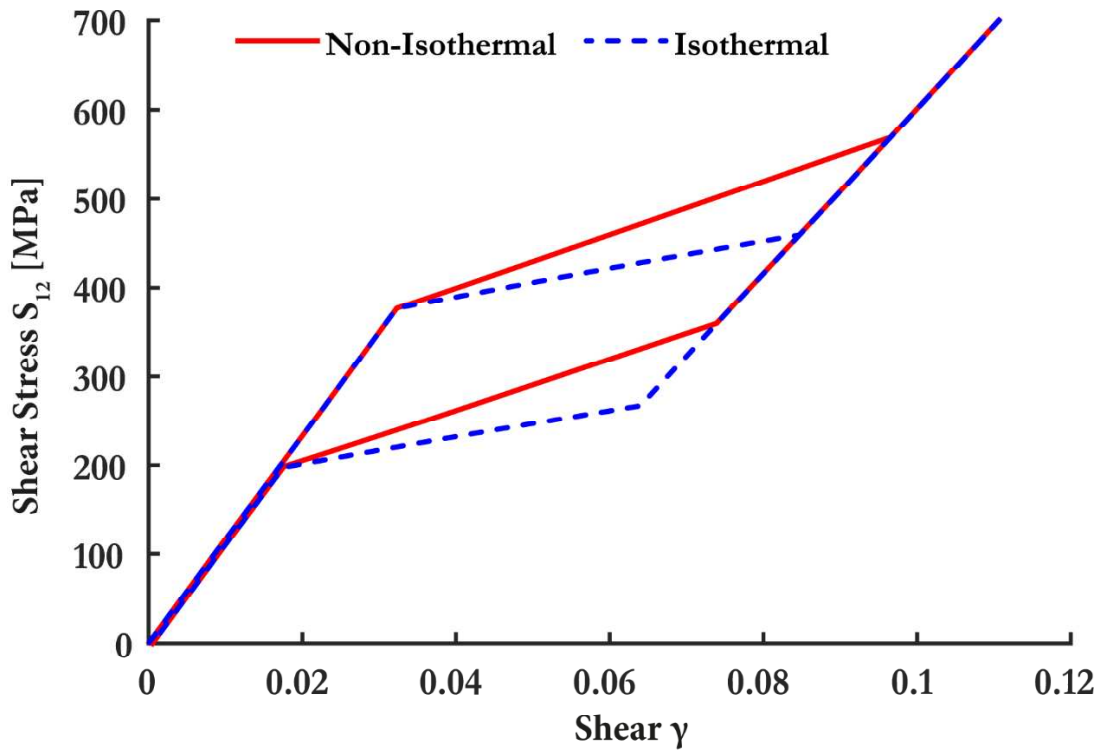
Figure 5: Finite Shear: Comparison of isothermal and adiabatic responses.

1058   Shear stress S_{12} vs. shear strain γ.
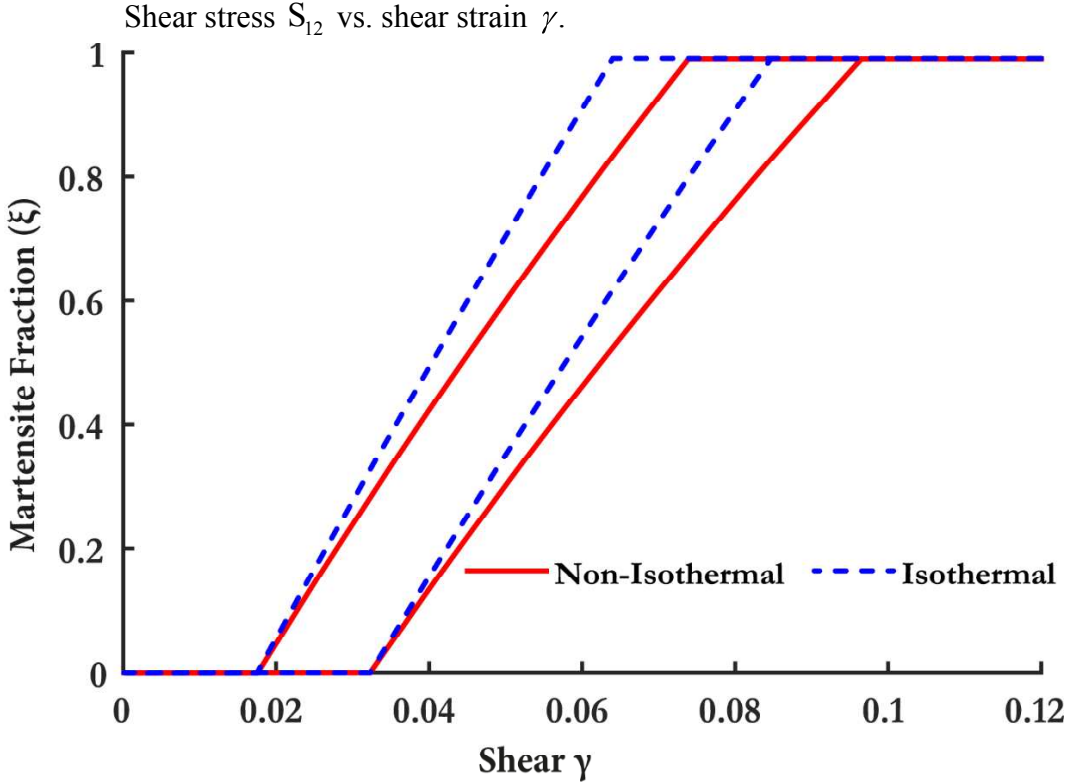
1059

1060

1061   Figure 6: Finite Shear: Comparison of isothermal and adiabatic responses.

1062   Martensite fraction ξ vs. shear s

1063
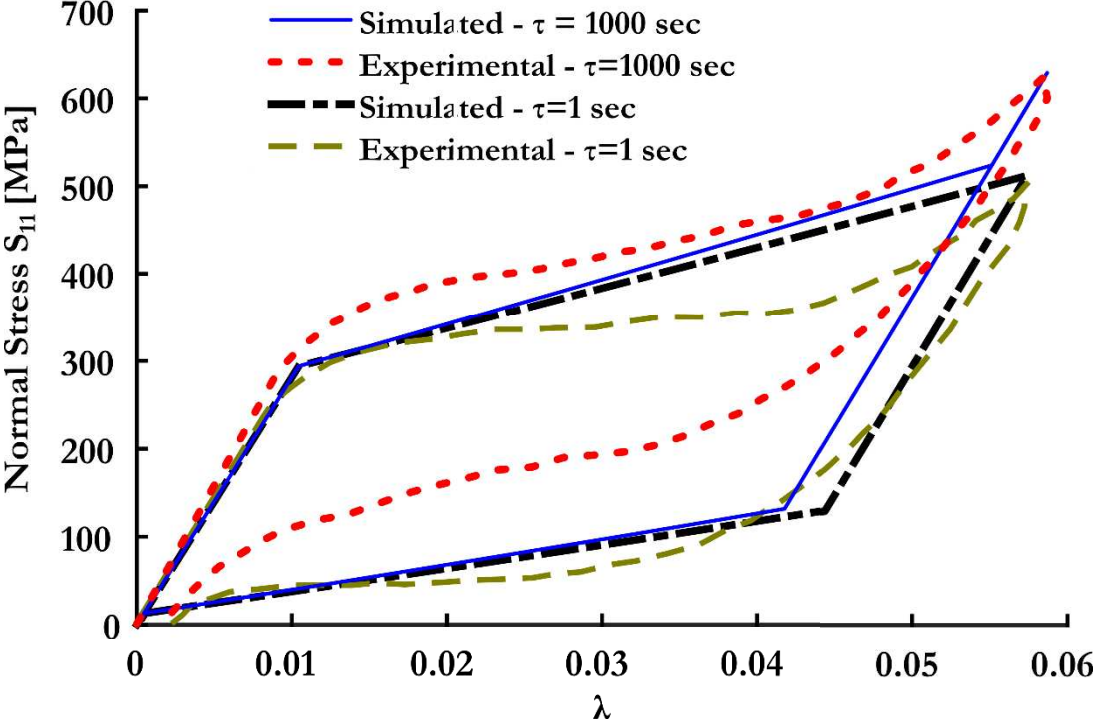
1064

1065   Figure 7: Comparison to experimental results: normal stress vs normal strain response

52
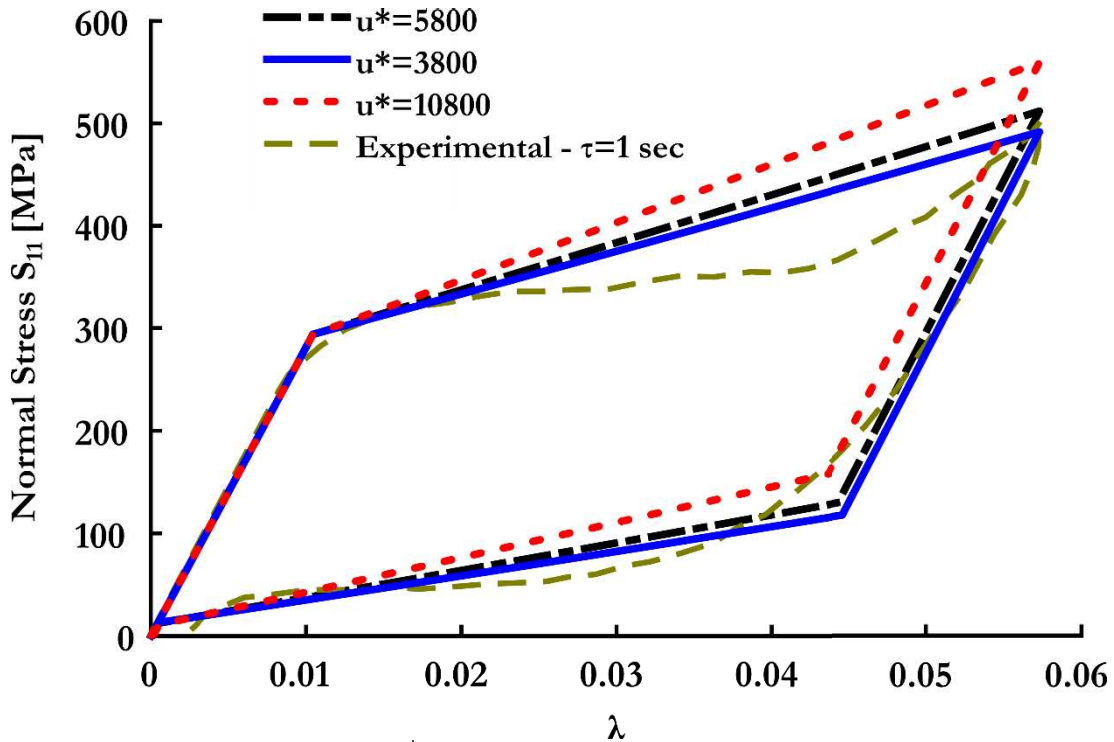
1067 Figure 8: Effect of parameter u*: normal stress vs normal strain response.
1068
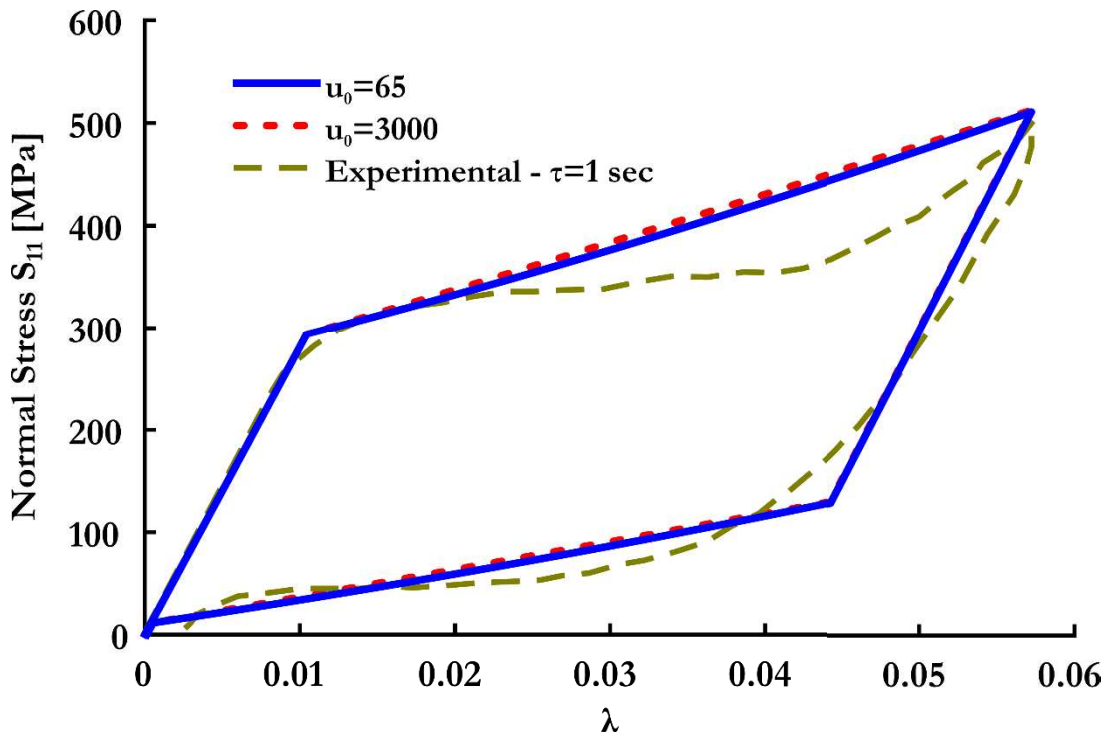
1069
1070 Figure 9: Effect of parameter u$_0$: normal stress vs normal strain response.
1071
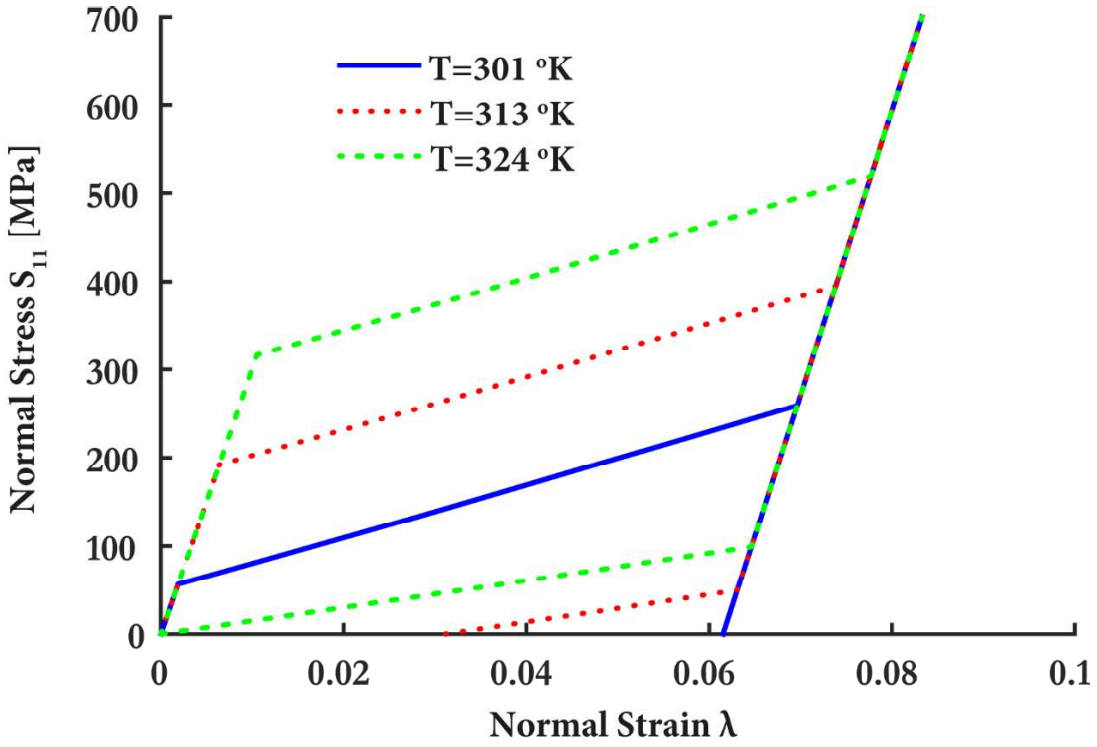
Figure 10: Uniaxial tension: Loading-unloading at different temperatures
Normal stress S_{11} vs. Normal strain λ.
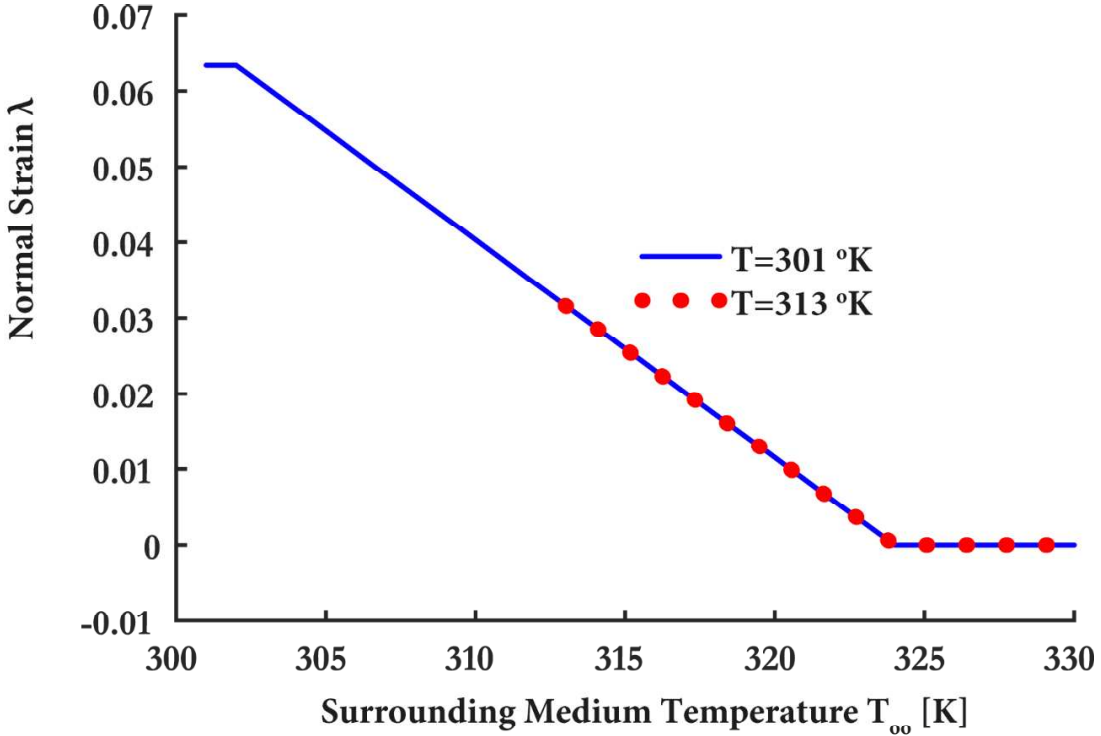
Figure 11: Shape memory effect: Normal strain λ vs. Surrounding medium temperature.

54
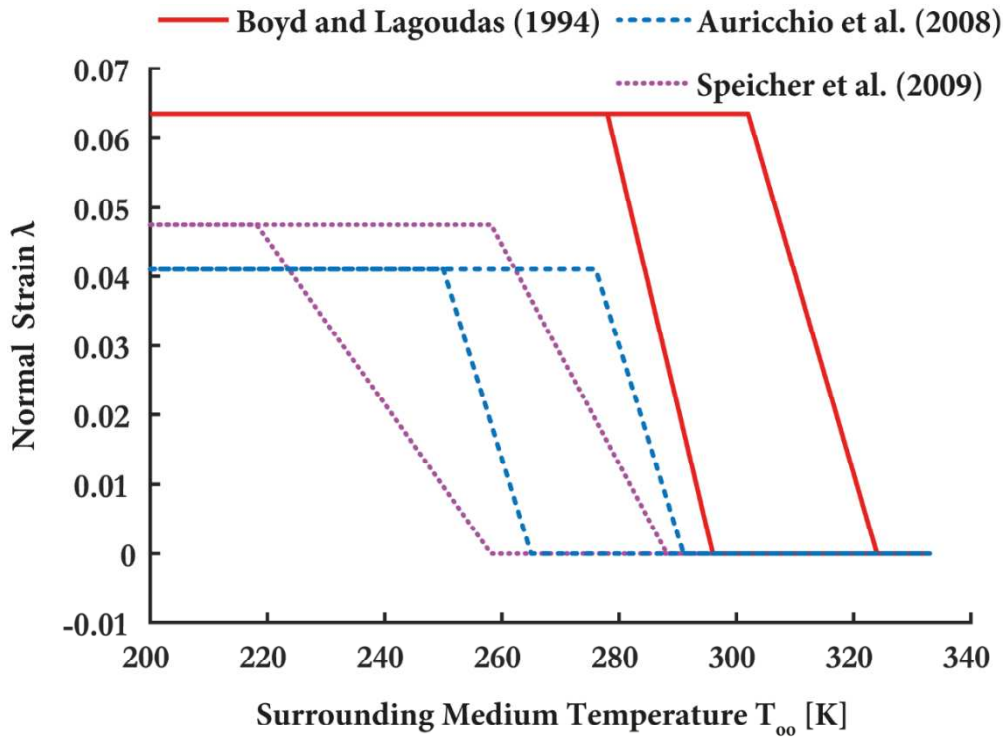
Figure 12: Temperature induced phase transformations: Normal strain λ vs. Surrounding medium temperature
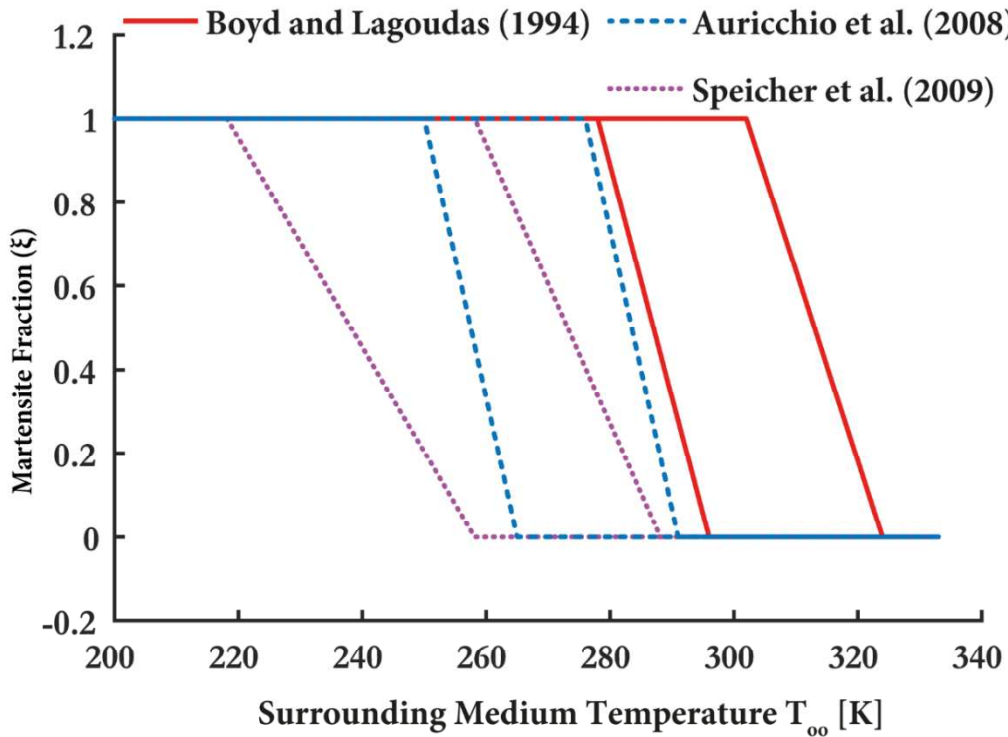
Figure 13: Temperature induced phase transformations: Martensite fraction ξ vs. Surrounding medium temperature
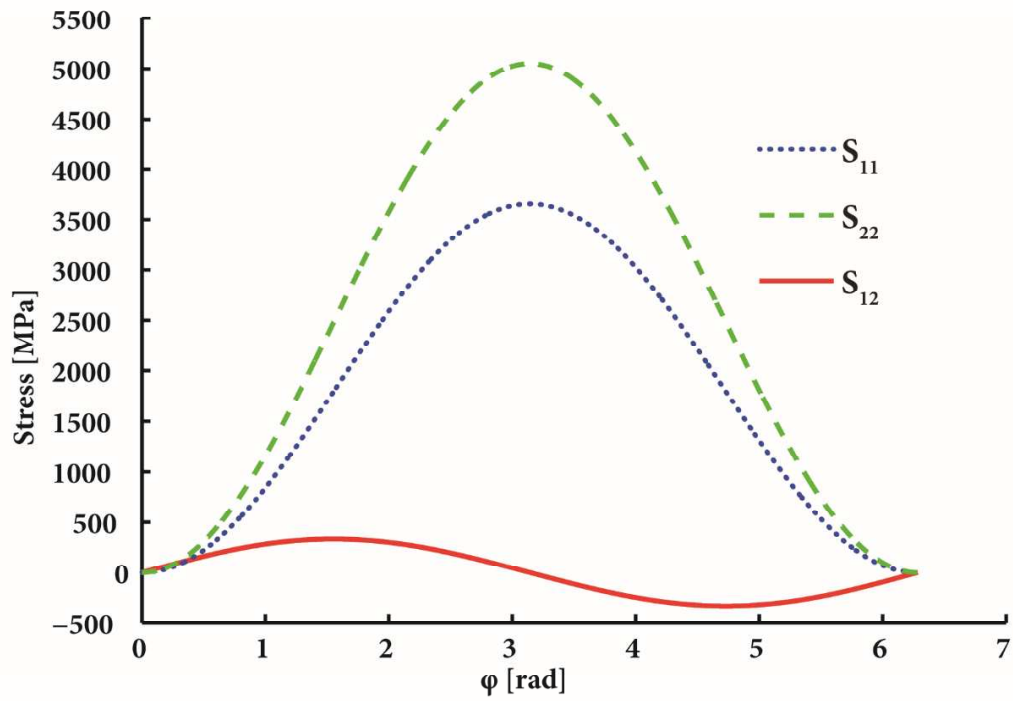
Figure 14: Response under a strain cycle: Stresses S_{11}, S_{12}, S_{22} vs. rotation angle φ.
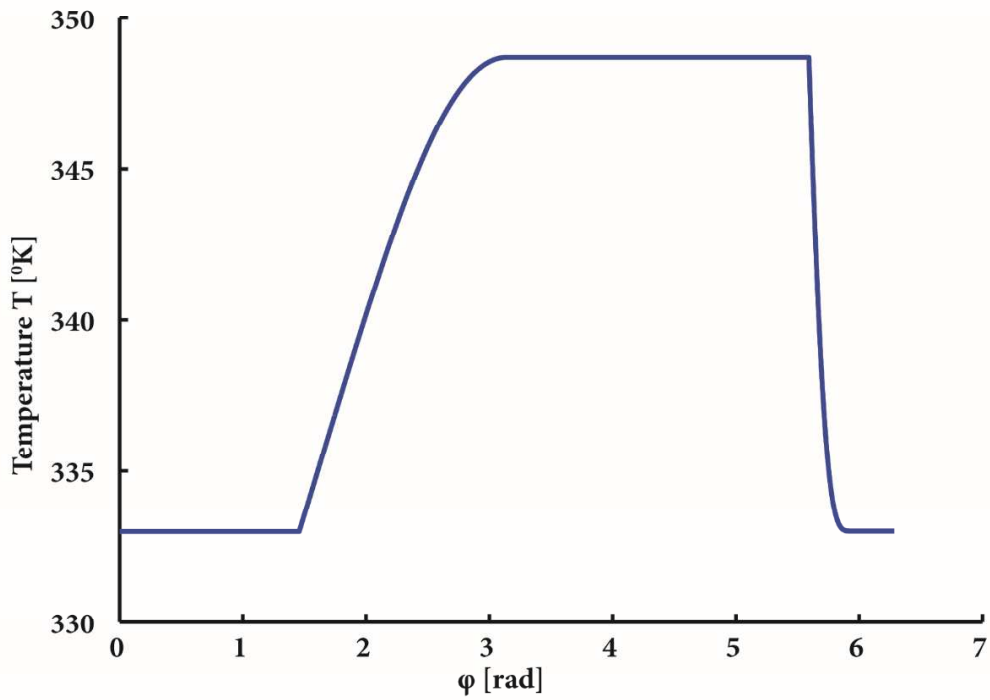
Figure 15: Response under a strain cycle: Temperature T vs. rotation angle φ.

56
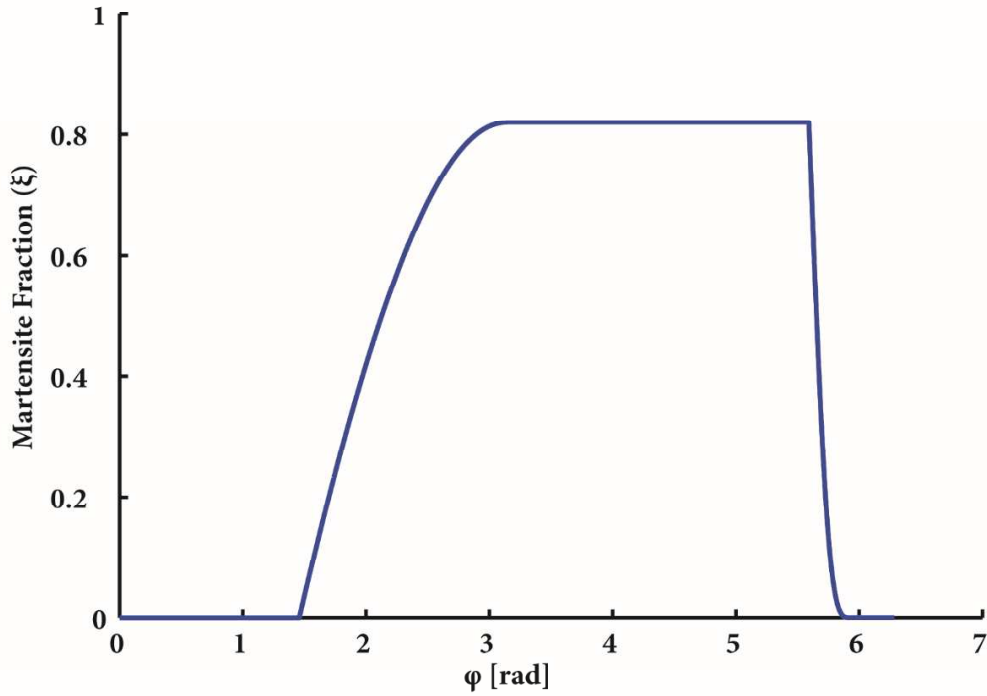
Figure 16: Response under a strain cycle: Martensite fraction ξ vs. rotation angle φ.
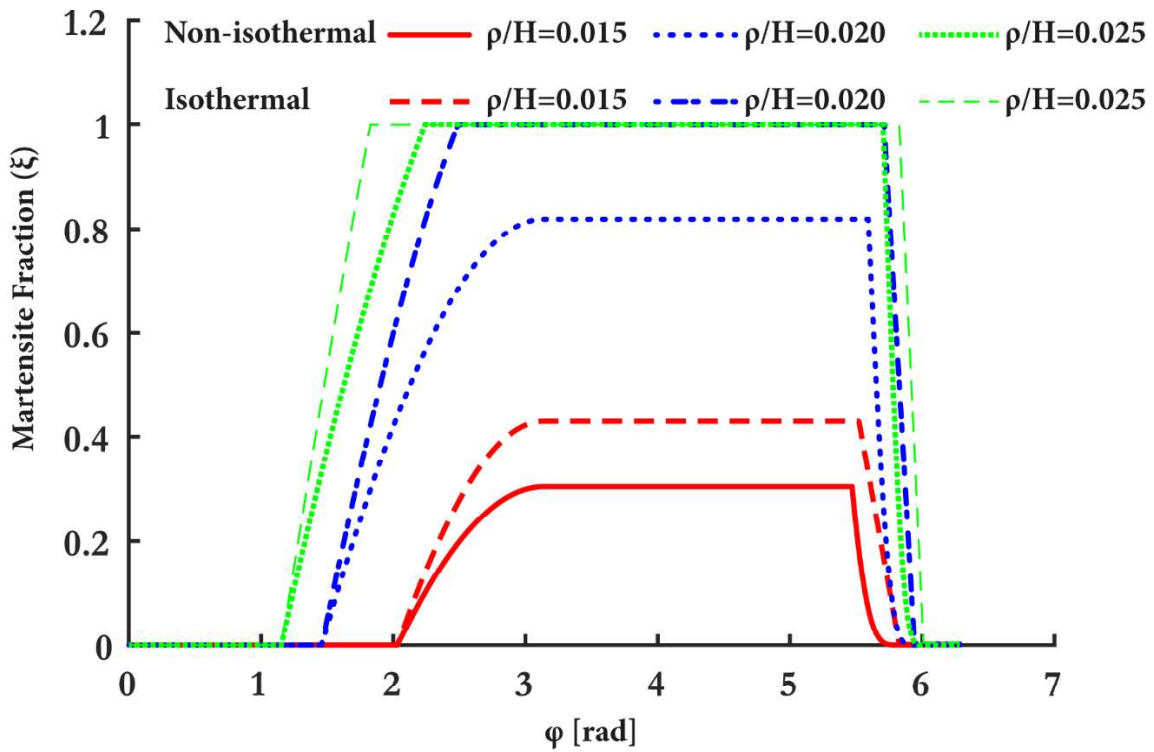
Figure 17: Response under a strain cycle: Comparison of isothermal and adiabatic responses. Martensite fraction ξ vs. rotation angle φ.
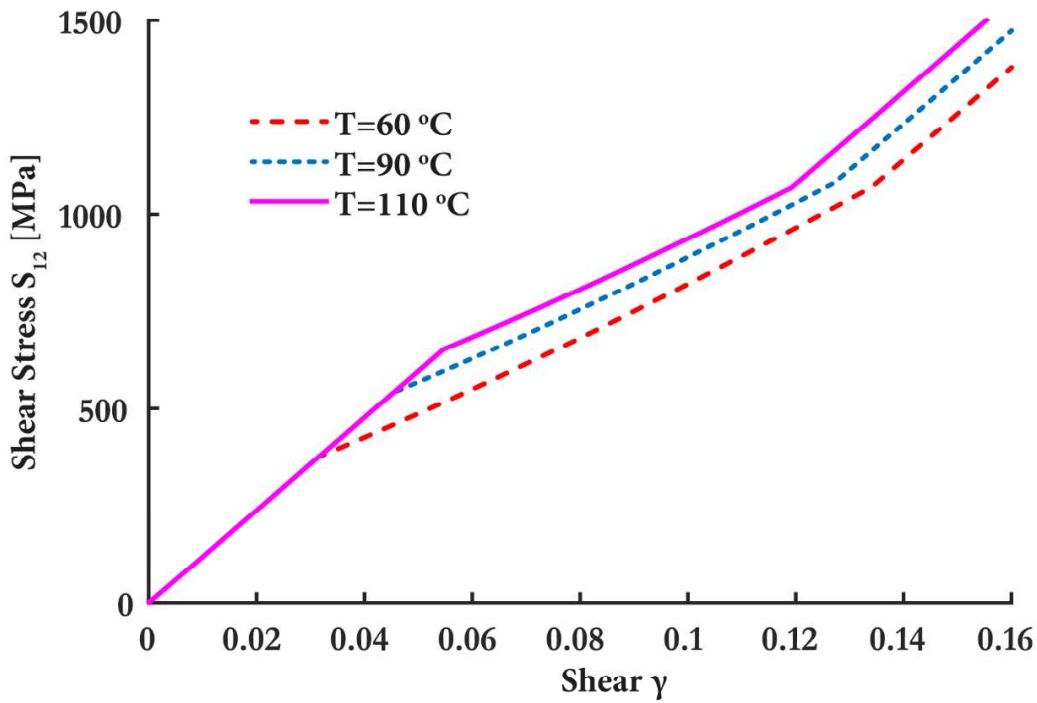
1099

1100   Figure 18: Finite Shear: Loadingat high values of the ambient temperature;
1101   Shear stress S_{12} vs. shear strain γ.
1102
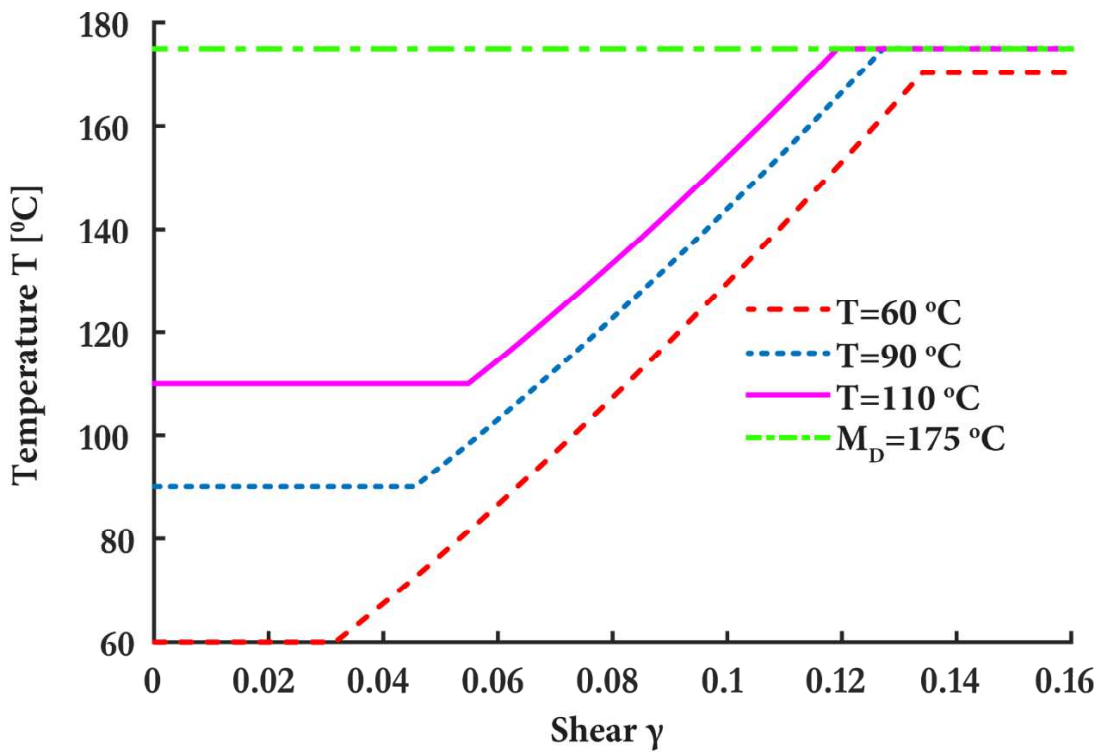
1103

1104   Figure 19: Finite Shear: Loadingat high values of the ambient temperature;
1105   Temperature T vs. shear strain γ.
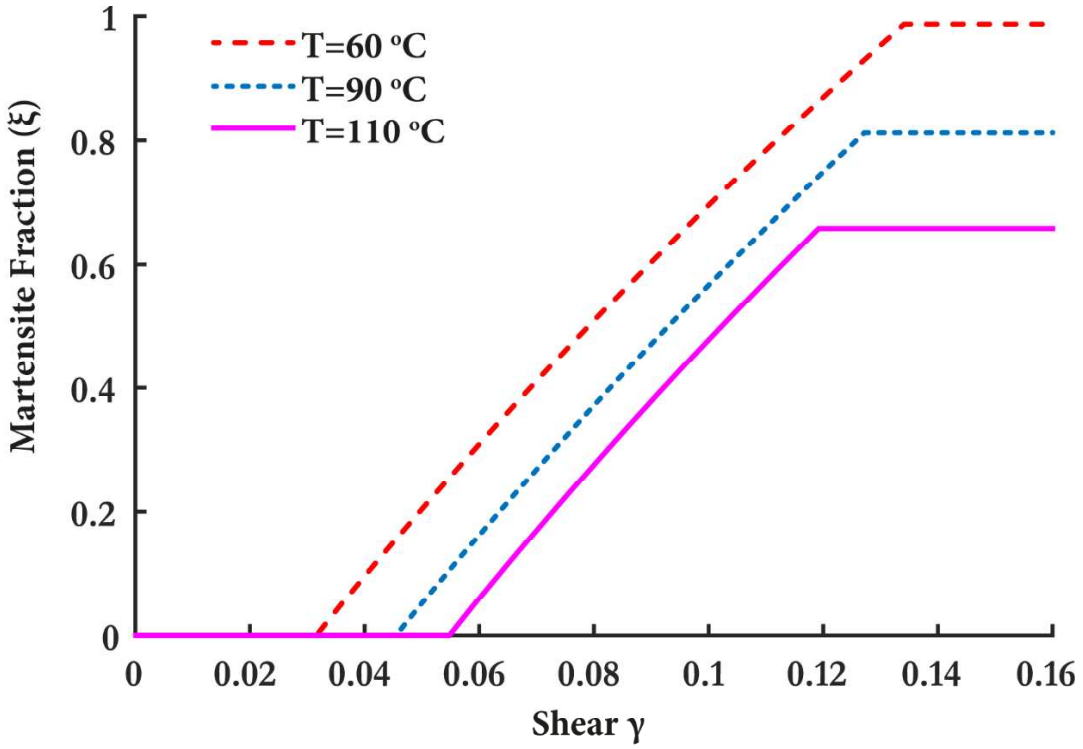
Figure 20: Finite Shear: Pseudoelastic behavior at high values of the material Martensite fraction ξ vs. shear strain γ.
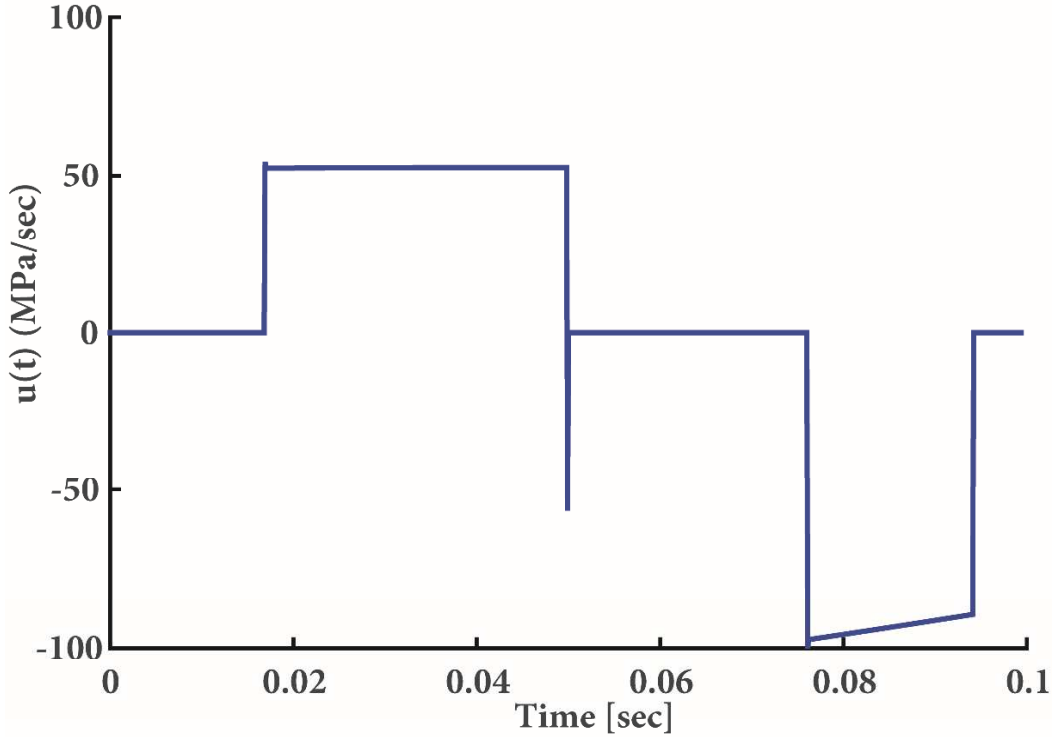
Figure 21: Thermomechanical response of a wire in uniaxial tension: Thermomechanical heat source $u(t)$ vs. time
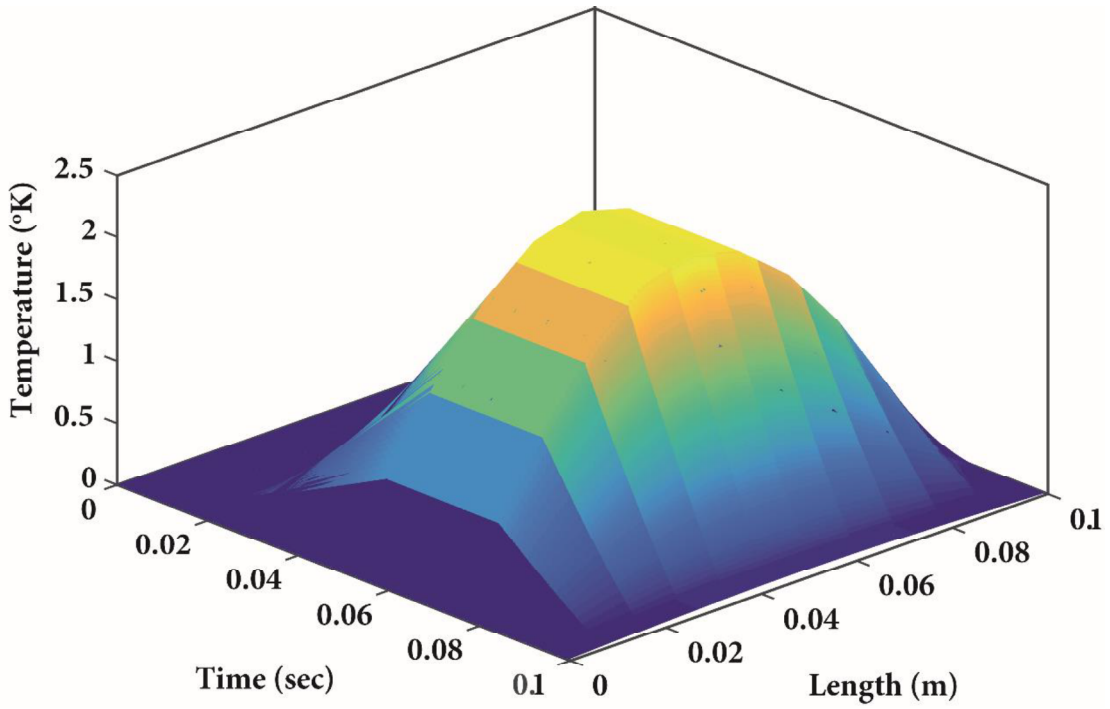
1113

1114 Figure 22: Thermomechanical response of a wire in uniaxial tension:
1115   Temperature evolution vs. time along the length of the wire

1116
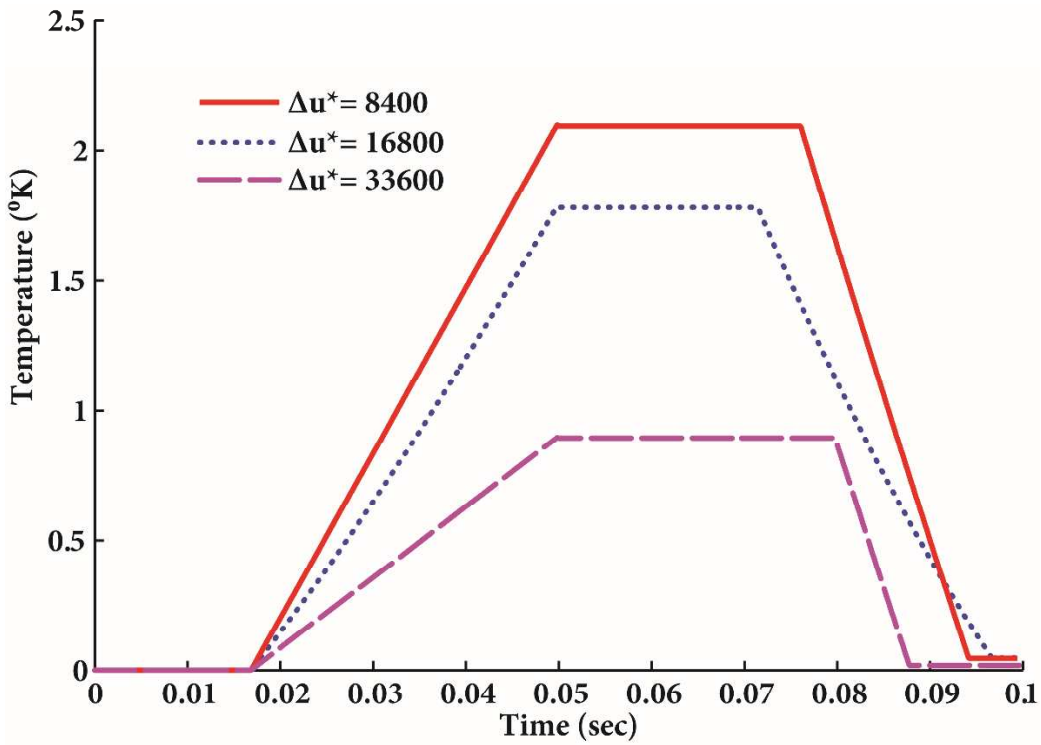
1117

1118 Figure 23: Thermomechanical response of a wire in uniaxial tension:
1119   Temperature evolution vs. time at the mid − point of the wire (Effect of the

1
2
3
4
5 1120   thermal parameter Δu^*)
6 1121
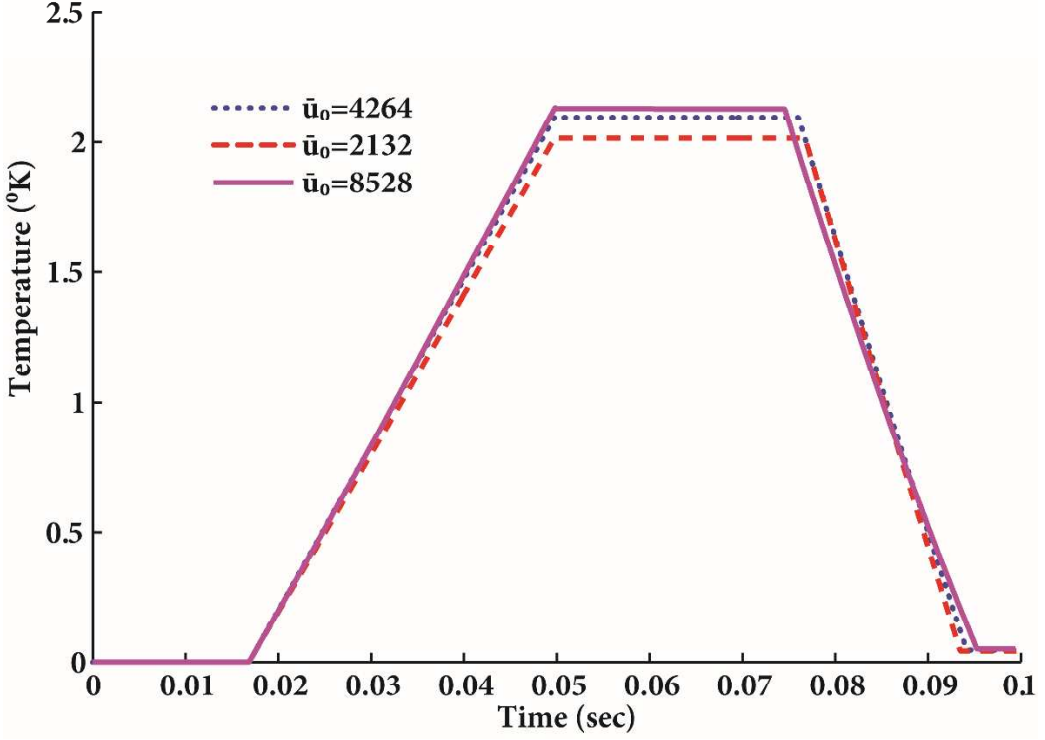
31 1122
32 1123   Figure 24: Thermomechanical response of a wire in uniaxial tension:
33 1124   Temperature evolution vs. time at the mid-point of the wire (Effect of the
34
35 1125   thermal parameter $\overline{u}_0$)